Reprogramming of the cardiac phosphoproteome in conjunction with proteome and transcriptome creates the enhanced performance and protection circuitry in response to chronic adenylyl cyclase-driven stress

Jia-Hua Qu, Khalid Chakir, Kirill V. Tarasov, Daniel R. Riordon, Maria Grazia Perino, Allwin Jennifa Silvester, and Edward G. Lakatta *

Laboratory of Cardiovascular Science, Intramural Research Program, National Institute on Aging, National Institutes of Health, Baltimore, MD 21224, USA.

Address correspondence to:

Dr. Edward G. Lakatta*

Laboratory of Cardiovascular Science

Intramural Research Program

National Institute on Aging

National Institutes of Health

251 Bayview Boulevard

Suite 100

Baltimore, MD 21224

USA.

Tel: +1 410-558-8202

lakattae@grc.nia.nih.gov

Abstract

Our previous work demonstrated the existence of a remarkable adaptive paradigm of heart performance and protection in response to the constitutive challenge of marked cardiac-specific overexpression of adenylyl cyclase type 8 (TGAC8). However, the molecular regulatory mechanisms remain elusive. Because PKA signaling is the predominantly activated pathway in the TGAC8 left ventricle (LV) performance and protection circuitry and phosphorylation related pathways were enriched from transcriptome and proteome, we hypothesized that phosphorylation states of numerous proteins are reprogrammed in pathways where the transcriptome and proteome were activated in TGAC8 vs. WT. We conducted an unbiased phosphoproteomics analysis in order to determine the role of altered protein phosphorylation in the chronic adaptive heart performance and protection profile of adult TGAC8 LV at 3-4 months of age, and integrated the phosphoproteome with transcriptome and proteome. Based on differentially regulated phosphoproteins by genotype, numerous stress-response pathways within reprogrammed TGAC8 LV, including PKA, PI3K and AMPK signaling pathways, predicted upstream regulators, e.g., PDPK1, PAK1 and PTK2B, and downstream functions, e.g., cell viability, protein quality control, and metabolism were enriched. In addition to PKA, numerous other kinases and phosphatases were hyper-phosphorylated in TGAC8 vs. WT. Hyper-phosphorylated transcriptional factors in TGAC8 were associated with increased mRNA transcription, and immune responses and metabolic pathways. Combination of the phosphoproteome with its proteome and with the previously published TGAC8 transcriptome enabled the elucidation of which cardiac performance and adaptive protection profiles were coordinately regulated at post-translational modification (PTM) (phosphorylation), translational and transcriptional levels. Many stress-response signaling pathways, i.e., PI3K/AKT, ERK/MAPK and ubiquitin labeling, were consistently enriched and activated in the TGAC8 LV at transcriptional, translational and PTM levels. We verified some results through wet lab experiments. Thus, PTM of protein by phosphorylation, per se, contributes immensely to the heart performance and protection profile of TGAC8 LV, and is coordinately regulated with altered transcription and translation in the TGAC8 to activate critical stress-response pathways.

Keywords

left ventricle, adenylyl cyclase 8, AC-cAMP-PKA-Ca^{2+} signaling, phosphoproteome, proteome, transcriptome, PI3K/AKT signaling pathway.

Introduction

Cyclic AMP (cAMP) is a pivotal second messenger, which exerts multifaceted effects on most significant physiological processes, such as cardiac contractility, glycogenolysis and lipolysis, hormone release, etc[1]. In mammalians, there are nine transmembrane adenylyl cyclase (AC) (mAC) isoforms (AC1-9) and one soluble AC (sAC, also called AC10) catalyzing the conversion of ATP into cAMP[2], which usually activates the phosphorylation cascade, serving as the central

motif of cellular signaling[1,3]. Increased AC-cAMP-PKA-Ca^{2+} signaling is the quintessential component of both acute and chronic cardiac responses.

AC8, the isoform, is highly expressed in brain regions[2,4]. Unlike two dominant cardiac AC isoforms, AC5 and AC6, which are inhibited by intracellular Ca^{2+} and inhibited in heart failure (HF), AC8 is stimulated by Ca^{2+}-calmodulin (CM)[5,6] and involved in nervous system functions, like learning and memory[2,4]. Our lab and others have demonstrated that cardiac-specific overexpression of AC8 (TGAC8) markedly increases the heart rate and ejection fraction, similar to acute exercise but chronic and in the absence of corporal exertion, and persists on a 24 hours per day and 7 days per week basis[5,7-9]. Despite this persistent high-level of heart performance driven by markedly elevated level of AC8-cAMP-PKA-Ca^{2+} signaling, which usually proceeds to near-term cardiac dysfunction, the TGAC8 survives for an extended period of time, up to about one year of age without excessive mortality.

It is of utmost importance to unravel how the TGAC8 adapts the heart to this chronic stress, as this knowledge can be applied to the study of cardiac physiology and pathology and even to develop treatments for cardiovascular diseases (CVDs). In this regard, as a first "port-of-call", we had recently compared the left ventricle (LV) transcriptome and proteome in TGAC8 and WT littermates[10]. Because PKA signaling pathway was highly enriched in TGAC8 vs. WT, we reasoned that protein phosphorylation will differ between TGAC8 and WT, and the phosphorylation modification will play a crucial role in the remarkable adaptation capacity of the TGAC8 heart in response to markedly increased AC8-cAMP-PKA-Ca^{2+} signaling. We have assessed the concordance of the genotypic differences at the phosphorylation level to some degree in western blot (WB) experiments[10].

As the body is a quite complex system, regulation at a single level cannot reveal the whole picture in an organism, and multiple levels of regulatory mechanisms are coordinated to defend against stimuli and maintain health[11]. Phosphorylation is one of the most important and most extensively studied post-translational modifications (PTMs) on proteins. Various kinases and phosphatases within cells phosphorylate and dephosphorylate a myriad of proteins respectively to regulate their activities and affect multiple signaling pathways. In the present research, we conducted Tandem Mass Tag (TMT)-labeling mass spectrometry (MS) of left ventricular samples of the three-month old male TGAC8 and WT mice, to unravel the reprogrammed phosphoproteome and proteome of the TGAC8 LV. In addition, by comparing genotypic differences in the proteome and phosphoproteome of the present study with genotypic differences in transcriptome published previously[10], we sought to determine whether some adaptive mechanisms that emerge in the TGAC8 LV are regulated at transcriptional, translational and PTM (phosphorylation) levels.

Materials and Methods

1. Animals.

The cardiac-specific overexpression of AC8 (TGAC8) mouse, generated by inserting a cDNA coding for human AC8 after the murine α-myosin heavy chain promoter, was a gift from Nicole Defer/Jacques Hanoune, Unite de Recherches, INSERM U-99, Hôpital Henri Mondor, F-94010 Créteil, France. The three-month old male TGAC mice were used as study cases, and age matched WT littermates, in the C57/BL6 background, were used as controls. All studies were performed in accordance with the Guide for the Care and Use of Laboratory Animals published by the National Institutes of Health (NIH Publication no. 85-23, revised 1996). The experimental protocols were approved by the Animal Care and Use Committee of the National Institutes of Health (protocol #441-LCS-2016).

2. Isolate and store mouse heart.

Three-month old male C57 mice (TGAC8 and WT) were euthanized and the heart was isolated. The left ventricle (LV) tissues were extracted and stored in tubes at -80°C.

3. Mass spectrometry for phosphoproteome and data process.

TGAC8 and WT LVs were sent to National Heart, Lung, and Blood Institute, National Institutes of Health, Bethesda to conduct mass spectrometry using the standard tandem mass tag (TMT) labeling method to obtain the phosphoproteome and total proteome concurrently in the same platform. Mass spectrometry manipulation referred to our recently published paper[10].

Proteins from each group of samples are being quantified using the Bradford Assay Kit. Two-hundred micrograms of protein from each group will be labeled with Amine-Reactive Tandem Mass Tag Reagents (TMT Label Reagents; Thermo Scientific) according to the protocol supplied by the manufacturer. Briefly, protein will be denatured followed by reduction (TCEP) and alkylation (iodoacetamide) and then the alkylated proteins (200ug) for each sample were precipitated in 6 volumes of ice-cold acetone at -20 °C overnight and later reconstituted in Triethylammonium bicarbonate. Each sample was digested overnight using Trypsin enzyme (enzyme to substrate ratio of 1:12.5) to get the peptide solution. Trypsin will cleave proteins at lysine and arginine amino acid residues yielding tryptic peptides.

The 10-plex tandem mass tag (TMT) labeling was carried out according to Thermo Fisher Scientific's TMT Mass Tagging kits protocol. Each of the TMT 10-plex label reagents were reconstituted in Acetonitrile (ACN) and digested peptides from each sample were incubated with specific tags (126, 127N, 127C, 128N, 128C, 129N, 129C, 130N,130C and 131 respectively) for about 1 hour at room temperature. The TMT labeled samples are then combined and fractionated

131 using Off-Line high pH Basic Reverse Phase Fractionation to decrease the complexity of the
132 sample and to increase the number of peptides being identified into a total of 24 fractions which
133 will be later analyzed using LC-MS/MS. About 5% of the labeled tryptic peptides from each of
134 24-fractions were used for global proteomics analysis by nanoLC-MS/MS analysis while the
135 remaining 95% of samples in the 24-fractions were subjected to subsequent TiO2-enrichment for
136 quantitative phosphoproteomics analysis.

137 TiO2 enrichment was conducted using a Titansphere Phos-kit (GL biosciences Inc.). The TMT
138 10-plex tagged tryptic peptides were reconstituted in Buffer B (25% lactic acid in 1% TFA, 80%
139 Acetonitrile). The TiO2 SpinTip (1mg resin/10ul tip) was incubated with the sample, washed
140 using the wash buffer following manufacturers protocol and the phosphopeptides were eluted in
141 elution buffer sequentially using 5% ammonium hydroxide solution and 5% pyrrolidine solution.
142 The eluted fraction was dried and reconstituted in 0.1% FA for subsequent clean-up using the
143 ZipTip C18-tips (Millipore). The sample from elution fraction of C18-tips were dried and
144 reconstituted in 0.1%FA for LC-MS/MS analysis.

145 The flow-through fraction and the wash fraction from the TiO2 spinTip was collected, pooled
146 into a total of 6 fractions and speedvac dried which will be later used for Fe-IMAC
147 phosphoenrichment protocol. The peptide sample from 6-pooled flow-through fractions from
148 TiO2 enrichment underwent second round of phosphoenrichment using High-Select Fe-NTA
149 Phosphopeptide Enrichment Kit (Thermo Scientific). The eluted fraction was dried and
150 reconstituted in 0.1% FA for subsequent LC-MS/MS analysis.

151 Protein identification by LC-MS/MS analysis of peptides was performed using an Orbitrap
152 Fusion Lumos Tribid mass spectrometer (Thermo Fisher Scientific, San Jose, CA) interfaced
153 with an Ultimate 3000 Nano-HPLC apparatus (Thermo Fisher Scientific, San Jose, CA).
154 Peptides were fractionated by EASY-Spray PepMAP RPLC C18 column (2µm, 100A, 75 µm x
155 50cm) using a 120-min linear gradient of 5-35% ACN in 0.1% FA at a flow rate of 300 nl/min.
156 The instrument was operated in data-dependent acquisition mode (DDA) using FT mass analyzer
157 for one survey MS scan on selecting precursor ions followed by top 3 second data-dependent
158 HCD-MS/MS scans for precursor peptides with 2-7 charged ions above a threshold ion count of
159 10,000 with normalized collision energy of 37%. Survey scans of peptide precursors from 300 to
160 2000 m/z were performed at 120k resolution and MS/MS scans were acquired at 50,000
161 resolution with a mass range m/z 100-2000.

162 All MS and MS/MS raw spectra of TMT experiments from each set were processed and searched
163 using Sequest HT algorithm within the Proteome Discoverer 2.2 (PD2.2 software, Thermo Fisher
164 Scientific).The settings for precursor mass tolerance was set at 12 ppm, fragment ion mass
165 tolerance to 0.05 Da, trypsin enzyme with 2 mis cleavages with carbamidomethylation of
166 cysteine, TMT6-plex (lysine), TMT6-plex (peptide N-term) as fixed modification and
167 deamidation of glutamine and asparagine, oxidation of methionine as variable modifications.
168 The mouse sequence database from Swiss sprot was used for database search. Identified peptides

were filtered for maximum 1% FDR using the Percolator algorithm in PD 2.2 along with additional peptide confidence set to high. Only peptide spectra containing all reporter ions were designated as "quantifiable spectra" and used for peptide/protein quantitation. The final lists of protein identification/quantitation were grouped and further filtered by PD 2.2 with at least 2 unique peptides per protein identified with high confidence. The quantitative protein ratios were weighted and normalized by the median ratio for all quantifiable spectra of the peptides pertaining to total protein identified.

For quantitative phosphopeptides analysis, an additional phosphorylation on Ser, Thr, Tyr residues were specified as variable modifications. To confidently localize phosphorylation sites, the phosphoRS 3.0 node integrated in PD 2.2 workflow was used. The algorithm of phosphoRS 3.0 software enables automated and confident localization of phosphosites by determining individual probability values for each putatively phosphorylated site within the validated peptide sequences. For each relative ratio group of phosphopeptides/sites, no normalization was applied.

To remove low quality signal, we remained peptides tagged with the medium and high confidence. We divided the expressions of phosphoproteins to those of total proteins to obtain the normalized phosphoproteome. As the expressions appeared to be near normal distribution, we calculated the fold change by dividing the average value of TGAC8 samples by the average value of WT samples, and calculated p-value using two-sided unpaired Student's t-test. Data were deposited in MassIVE (ID: MSV000089850).

4. Analyses of the TGAC8 LV transcriptome.

The processed transcriptomic data were obtained from our recently published work (GEO: GSE205234)[10]. The significantly changed mRNAs (TGAC8 vs. WT, q-value < 0.05) were uploaded into DAVID[2] (version: 6.8; https://david.ncifcrf.gov/home.jsp) for Gene Ontology (GO) term enrichments, and were also imported into Ingenuity Pathway Analysis[3] (IPA (QIAGEN, March 2020)) for upstream kinases and phosphatases prediction. Kinases and phosphatases were selected from the transcriptome and their changes at mRNA level were displayed to observe their regulation by the overexpression of AC8.

5. Analyses of phosphoproteome and proteome.

Both unnormalized and normalized phosphoproteome were analyzed and visualized in PCA, heatmap, and volcano plots. With the cutoff -log(p-value) > 1.3 and absolute(log2(fold change)) ≥ 0.4, we obtained the significantly changed unnormalized and normalized phosphoproteins (TGAC8 vs. WT) and imported them into IPA for functional analyses respectively, and compared the canonical pathway enrichments from these two datasets. In IPA, the upstream kinases were predicted based upon the unnormalized phosphoproteom, and the regulatory

205 pathways from the predicted upstream kinases to downstream effective signaling pathways were
206 generated. Molecular and cellular functions were also enriched in IPA. The similar analyses to
207 those conducted in the TGAC8 LV transcriptome were also done in the TGAC8 LV total
208 proteome to observe the GO term enrichment, predicted activities of upstream kinases and
209 phosphatases, and expression of kinases and phosphatases at protein level.

210

211 **6. Analyses of phosphopeptides.**

212 The upregulated phosphopeptides (TGAC8 vs. WT, p-value < 0.05 and log2(fold change) > 0)
213 were processed in R. After split of peptides with multiple phosphosites into individual peptides
214 and filtering of ambiguously identified sites, 2264 phosphopeptides were selected. Protein
215 peptide sequences of full length were downloaded from Uniprot database[12] and matched to the
216 protein accessions corresponding to processed and selected phosphopeptides. Peptides centered
217 on the phosphosites and flanked by 6 amino acids on the N and C termini respectively were
218 extracted from the matched protein peptide sequences, and uploaded into WebLogo[13]
219 (http://weblogo.threeplusone.com/) and iceLogo[14] (https://iomics.ugent.be/icelogoserver/) for
220 sequence motif analysis. In WebLogo online analysis, different amino acids were labeled in
221 different colors representing different chemical properties (refer to figure legend). In iceLogo
222 online analysis, a public amphiphilicity index of polar amino acids reported by Mitaku and
223 colleagues[15] was used as an aid to characterize the amino acid preference at membrane-water
224 interfaces. In addition, the phosphopeptides of PI3K/AKT substates were summarized and
225 displayed in stacked bar plot.

226

227 **7. Integrative analyses of transcriptome, proteome and phosphoproteome.**

228 The changes of significantly regulated molecules (TGAC8 vs. WT, q-value or p-value < 0.05) in
229 transcriptome, total proteome, and unnormalized phosphoproteome were displayed in circos plot.
230 In addition, the changes at different level were compared and visualized in correlation scatter
231 plots. The discordant proteins whose change directions in total proteome and phosphoproteome
232 were opposite were used to analyze the specific regulation at the phosphorylation level by the
233 use of Reactome and GO (Cellular Component and Biological Process) databases.

234 As to the coordinated regulation, the above mentioned significantly regulated molecules
235 (TGAC8 vs. WT) in each dataset were imported into IPA for canonical pathway enrichment.
236 PI3K/AKT, ERK/MAPK and protein ubiquitination signaling pathways were coordinated across
237 all omics. The phosphopeptides of protein substrates of PI3K were extracted from the
238 phosphopeptide dataset and the numbers of changed phosphopeptides (TGAC8 vs. WT) were
239 summarized and visualized in stacked bar plot. The PI3K/AKT signaling pathway were
240 visualized in IPA, and nodes in the pathways were marked in different colors in terms of their
241 changes at different levels.

242 As kinases and phosphatases are pivotal in phosphorylation, and transcription factors (TFs) are
243 important in transcription regulation, they were extracted from transcriptome, proteome, and
244 phosphoproteome to observe their changes (TGAC8 vs. WT) and deduce their role in the
245 reprogram of phosphoproteome. The upstream transcription regulators including but not only
246 TFs were predicted on the basis of transcriptome and proteome by the utilization of knowledge
247 base in IPA, and their expressions were searched in multiple datasets. Furtherly, TFs that were
248 significantly regulated at phosphorylation level (TGAC8 vs. WT, p-value < 0.05) were defined
249 as significantly changed phosphorylated TFs in this research, and they were uploaded into
250 STRING database[4] (version: 11.0; http://string-db.org/) to generate protein-protein interaction
251 network and enrich KEGG pathways. They were also imported into IPA for canonical pathway,
252 molecular and cellular functions enrichments.

253

254 **8. Western blot.**

255 Snap-frozen left ventricle (LV) tissue from three-month-old male mice was homogenized and
256 lysed in ice cold RIPA buffer (Thermo Fisher Scientific: 25 mM Tris-HCl (pH 7.6), 150 mM
257 NaCl, 1% NP-40, 1% sodium deoxycholate, 0.1% SDS) supplemented with a Halt protease
258 inhibitor cocktail (Thermo Fisher Scientific), Halt phosphatase inhibitor cocktail (Thermo Fisher
259 Scientific) and 1 mM phenylmethyl sulfonyl fluoride, using a Precellys homogenizer (Bertin
260 Instruments) with tissue homogenization kit CKMix (Bertin Instruments) at 4 °C. Extracts were
261 then centrifuged at 10,000×g for 10 min at 4 °C and the protein concentration of the soluble
262 fraction determined using the Bicinchoninic Acid (BCA) Assay (Thermo Fisher Scientific).
263 Samples were denatured in Laemmli sample buffer (BioRad Laboratories) containing 355 mM 2-
264 mercaptoethanol at 95 °C for 5 min, and proteins (10–50 µg/lane) resolved on 4–20% Criterion
265 TGX Stain Free gels (Bio-Rad Laboratories) by SDS/PAGE. Gels then exposed to UV
266 transillumination for 2.5 min to induce crosslinking of Stain Free gel trihalo compound with
267 protein tryptophan residues. Proteins were then transferred to low fluorescence polyvinylidene
268 difluoride (LF-PVDF) membranes (BioRad Laboratories) using an electrophoretic transfer cell
269 (Mini Trans-Blot, Bio-Rad). Membrane total protein was visualized using an Amersham Imager
270 600 (AI600) (GE Healthcare Life Sciences) with UV transillumination to induce and a capture
271 fluorescence signal.

272 Blocked membranes (5% milk/tris-buffered saline with Tween-20, TBST) were incubated with
273 the following primary antibodies: (1) Anti-Phospho-PKA Substrate (RRXS*/T*) antibody, Cell
274 Signaling Technologies, Cat.#9624, 1:1000 dilution; (2) Anti-Ubiquitin antibody produced in
275 rabbit, Sigma-Aldrich, SAB1306582, 1:200 dilution; (3) Anti-pan-AKT antibody, Cell Signaling
276 Technologies, Cat.#4691, 1:1000 dilution; (4) Anti-Phospho-pan-AKT (Thr308) antibody, Cell
277 Signaling Technologies, Cat.#13038, 1:1000 dilution; (5) Anti-Phospho-pan-AKT (Ser473)
278 antibody, Cell Signaling Technologies, Cat.#4060, 1:1000 dilution; (6) Anti-AKT2 antibody,
279 Abcam, Cat.#13038, 1:1000 dilution; (7) Anti-Phospho-AKT2 (Ser473) antibody, Cell Signaling

280 Technologies, Cat.#ab131168, 1:1000 dilution; (8) Anti-ERK1/2 antibody, Cell Signaling
281 Technologies, Cat.#4695, 1:1000 dilution; (9) Anti-Phospho-ERK1/2 (Thr202/Tyr204) antibody,
282 Cell Signaling Technologies, Cat.#4376, 1:1000 dilution; (10) Anti-p21 Ras antibody, Cell
283 Signaling Technologies, Cat.#3965, 1:1000 dilution; (11) Anti-GAPDH antibody, Santa Cruz
284 Biotechnology, Cat.# sc-32233, 1:1000 dilution; (12) Anti-c-Raf antibody, ThermoFisher
285 Scientific, Cat.# PA5-29333, 1:1000 dilution; (13) Anti-Phospho-c-Raf (Ser338) antibody, Cell
286 Signaling Technology, Cat.# 9427, 1:1000 dilution; (14) Anti-MEK1/2 antibody, Cell Signaling
287 Technology, Cat.# 9126, 1:1000 dilution; (15) Anti-Phospho-MEK1/2 (Ser221) antibody, Cell
288 Signaling Technology, Cat.# 2338, 1:1000 dilution.

289 Primary antibodies were then detected using horseradish peroxidase (HRP) conjugated antibody
290 (Invitrogen) at 1:10,000. Bands were visualized using Pierce SuperSignal West Pico Plus ECL
291 substrate kits (Thermo Scientific), the signal captured using an Amersham Imager 600 (AI600)
292 (GE Healthcare Life Sciences) and quantified using ImageQuant TL software (GE Healthcare
293 Life Sciences). Band density was normalized to total protein. Two-tailed unpaired Student's t
294 test with Welch's correction was used for statistics.

295

296 **9. Protein synthesis detection.**

297 Protein synthesis was assessed by SUnSET-Western Blot as previously described in the above
298 section. Briefly, the puromycin solution was prepared in PBS, sterilized by filtration, and a
299 volume of 200 µl was injected in mice intraperitoneally, to achieve a final concentration of 0.04
300 µmol/g of body mass. After 30 min, mice were sacrificed, the LV was harvested and snap frozen
301 in liquid nitrogen. Protein extraction was performed using Precellys, quantified with BCA assay
302 25 µg of total protein were separated by SDS-PAGE; proteins were then transferred onto PVDF
303 membrane and incubated overnight in the anti-puromycin primary antibody (MABE343, Sigma-
304 Aldrich, St. Louis, MO). Visualization of puromycin-labeled bands were obtained using
305 horseradish peroxidase conjugated anti-mouse IgG Fc secondary antibody (Jackson
306 ImmunoResearch Laboratories Inc, West Grove, PA, USA), using Pierce Super Signal ECL
307 substrate kit (Pierce/ Thermo Scientific Rockford, IL). Chemiluminescence was captured with
308 the Imager AI600 and densitometry analysis was performed using ImageQuantTL software (both
309 by GE, Boston, MA). Total protein was used as control for protein loading. Genotypic
310 differences of protein synthesis were tested via an as unpaired t-test.

311

312 **10. Proteasome activity detection.**

313 Flash frozen tissue was homogenized in ice-cold cytosolic extraction buffer (50 mM Tris-HCl
314 pH 7.5, 250 mM Sucrose, 5 mM MgCl2, 0.5 mM EDTA, and 1 mM DTT). A bicinchoninic acid
315 (BCA) assay (Pierce) was used to determine the protein concentrations. All samples were equally
316 concentrated in proteasome assay buffer (50 mM Tris-HCl pH 7.5, 40 mM KCl, 5 mM MgCl2,

317 and 1 mM DTT). Proteasome activity was determined in the presence of 28 μM ATP using the
318 Suc-LLVY-AMC (18 μM, Boston Biochem #S280) fluorogenic substrate with and without
319 proteasome inhibition (MG 132, 1 mM, Sigma). The plate was read at an excitation wavelength
320 of 380 nm and an emission wavelength of 469 nm using a Spectramax M5 (Molecular Devices).
321 Activity was calculated by subtracting the background (proteasome inhibited value) from the
322 reading (proteasome activated value).

323

324 **11. Protein soluble and insoluble fractions detection.**

325 Protein aggregates were measured using Proteostat (Enzo, ENZ-51023) following the
326 manufacturer's instructions. For this assay left ventricle myocardial lysate (Cell Signaling lysis
327 buffer) was obtained, protein concentration assayed (BCA assay [Pierce]). Ten μg of protein
328 loaded into a 96-well microplate and protein aggregates were analyzed using the Proteostat assay
329 kit (Enzo Life Sciences) following the manufacturer's instructions. Background readings were
330 subtracted from sample recordings and were normalized to wild-type values.

331

332 **12. Data process and graphics production.**

333 Most raw data were precleared and processed using RStudio (version: 1.1.463) in R language
334 (version: 3.5.3), in which the tidyr package and dplyr package were applied. In addition,
335 GraphPad Prism (version: 7), Microsoft Excel (version: 2019) and Adobe Illustrator (version:
336 CC 2019) were also used for statistics and graphics. Venn diagrams were generated in Venny[5]
337 (version: 2.1.0; http://bioinfogp.cnb.csic.es/tools/venny/index.html). Circos plot was generated
338 using Circos software[6] in Perl language.

339

340

341 **Results**

342 **1. The TGAC8 reprograms the LV phosphoproteome.**

343 The TMT-labeling quantitative MS identified **12963 phospho-peptides** (File 1: Sheet 1) and
344 **3646 phosphoproteins** (File 1: Sheet 2). The principal component analysis (PCA) (Figure 1A)
345 of the 3646 phosphoproteins in each mouse showed that the TG and WT samples were
346 distinguished into two groups completely. The heatmap (Figure 1B) showed the intra-group
347 consistency of upregulated phosphoproteins in TGAC8 compared to WT. Within the cutoff at -
348 log10(p-value) > 1.3 and absolute value of log2(fold-change(TG/WT)) ≥ 0.04, 781
349 phosphoproteins were differentially regulated by genotype. Of the 781 phosphoproteins, the
350 phosphorylation levels of 741 proteins were increased and only 40 were decreased in the TGAC8
351 vs. WT LV (Figure 1C).

352

353 **2. Functional analyses of the phosphoproteome.**

354 We performed the canonical pathway, upstream regulation, and downstream function analyses of
355 the remodeled LV phosphoproteome of TGAC8 using the Ingenuity Pathway Analysis (IPA)
356 software.

357 **2.1. Canonical pathway analysis of the remodeled LV phosphoproteome of TGAC8.**

358 To study the mechanism at phosphorylation level, we first performed canonical pathway analysis
359 using IPA. Top canonical pathways within the phosphoproteome that were statistically
360 differentially enriched in TGAC8 vs. WT were displayed in the bar plot (Figure 1D and File 2:
361 Sheet 1). Of these pathways, cardiac hypertrophy signaling (enhanced) is most highly activated
362 (z-score as high as 4.867) (Figure 1D). The combination of Supplementary Figure 1 and File 2:
363 Sheet 2 and our recently published work[10] showed that the phosphorylation status of numerous
364 molecules, e.g., Ca^{2+} ATPase, RyR2, Ncx, involved in excitation, calcium cycling, contraction,
365 relaxation and protein synthesis, was elevated in the TGAC8 vs. WT LV. However, we have
366 demonstrated that at three-month of age, the mouse age in the present study, the LV mass is not
367 elevated in TGAC8 vs. WT[10]. Of note, transcriptomic, proteomic and WB analyses indicated that
368 pathologic hypertrophic markers were not increased in TGAC8 vs. WT[10]. In this regard, the
369 activation of key stress response signaling pathways, e.g., protein kinase A (PKA) signaling,
370 PI3K signaling, and AMPK signaling, may protect against pathological changes, that result in an
371 increase in cardiac mass in TGAC8 despite its chronic increase in performance. For example,
372 activated PKA signaling can restrict the activity of AC8, acting as a feedback to fine-tune the
373 downstream signaling networks inside the body[3]. Additionally, nitric oxide (NO) signaling may
374 coordinate cardiac protection in the increase in cardiac mass (Figure 1D). Increased
375 phosphorylation status of HSP90 and Akt in TGAC8 synergistically increase eNOS activity[16],
376 and increased NO produced by eNOS may modulate the function of the ryanodine receptor Ca^{2+}
377 release channel (RyR2) on the cardiac sarcoplasmic reticulum[17]. The TMT-labeling MS
378 identified significant upregulated phosphorylation in the peptides of RyR2
379 (RISQTSQVSIDAAHGYSPR, E9Q401 [2805-2823]) (File 1: Sheet 1) , consistent with the PKA
380 induced phosphorylation of RyR2-S2809 mediating the increase in Ca^{2+} spark amplitude[18].

381 **2.2. Upstream regulators of the remodeled LV phosphoproteome of TGAC8.**

382 As known, the overexpression of AC8 activates the AC8-cAMP-PKA phosphorylation axis[9].
383 There were 2264 phosphosites whose names and locations are unambiguous within the 4990
384 upregulated phosphopeptides (p-value ≤ 0.05 and log2(fold-change(TG/WT)) ≥ 0) in TGAC8 vs.
385 WT. The majority of these phosphosites were serines (S) and threonines (T), and a few were
386 tyrosines (Y) (Figure 2A). By using WebLogo, we profiled the phosphorylation motif sequences
387 (Figure 2B). A typical PKA and AKT substate motif, R-R-X-pS/T, was the most abundant
388 substrate motif, consistent with increased PKA dependent phosphorylation (Figure 2B-2D)[19,20].

389 In addition to S and T, the center phosphosites also included phosphotyrosine (Y). The center
390 phosphosites were mainly flanked by the P-E-E sequence on the C terminus, endowing a strong
391 hydrophobic and acidic property to the C terminus of the substrate sequences (Figure 2B),
392 supported by the amphiphilicity index analysis in iceLogo (Figure 2D). Because phosphorylation
393 substrate motifs were not restricted to PKA's substrate motif, additional kinases must be also
394 involved in reprogramming the TGAC8 phosphoproteome. Therefore, we were inspired to
395 explore additional kinase-substrate pathways mediating the effect of the cardiac-overexpression
396 of AC8 here.

397 IPA predicted that 26 kinases were responsible for the above-mentioned phosphorylation motifs
398 (File 2: Sheet 3), among which, three had previously been identified to differ by genotype in the
399 LV transcriptome, 18 were shown to differ by genotype in the LV proteome, and 18 were
400 identified in the present phosphoproteome. Of note, most of the identified kinases were
401 upregulated in TGAC8 vs. WT at transcription, translation and PTM (phosphorylation) levels.
402 Within the phosphoproteome, eight kinases were predicted to be differentially activated by
403 genotype, and the phosphorylation level of four of these (PDPK1, PAK1, PTK2B and GSK3B)
404 was increased in TGAC8 vs. WT. These four kinases each phosphorylates various proteins to
405 regulate cellular functions. For example, a previous study observed that in human glioblastoma
406 cell lines, T98G and U87MG cells, the interference of human PDPK1 mRNA by siRNA
407 decreased the phosphorylation level of human BAD protein (S112, S136 and S155) and activated
408 cell death to suppress tumorigenesis[21]. Another study reported that in mouse myoblast cell line,
409 C2C12 cells, PDPK1 protein phosphorylated the mouse ULK1 protein[22]. Increased
410 phosphorylation states of BAD (upregulated at S112, S136 and S155) and ULK1 (upregulated at
411 S450, S521 and S637/638) in TGAC8 may be linked to activated PDPK1.

412 Different kinases can coordinate to reprogram the complex regulation network in the organism.
413 Consistent with the IPA canonical pathway analysis, the phosphorylation level of 27 proteins
414 (including the three kinases (PDPK1, PAK1 and PTK2B) auto-phosphorylating themselves)
415 were elevated by the three kinases to regulate cardiac stress signaling pathways, including PKA
416 signaling, ERK/MAPK signaling, cardiac hypertrophy signaling (enhanced), and renin-
417 angiotensin signaling (Figure 1E), to cope with the cardiac stress in the TGAC8. For example,
418 GSK3B is involved in multiple biological processes. PDPK1 phosphorylated GSK3B at S9[23,24]
419 and PTK2B phosphorylated GSK3B at S9 and Y216[25,26] to inhibit the kinase activity of GSK3B.
420 In this phosphoproteome, GSK3B was phosphorylated at multiple sites, including S9, Y216,
421 S219 and S545, and thus GSK3B inhibition was linked to the cardiac adaptation[27,28].

422 **2.3. Downstream functions of the remodeled LV phosphoproteome of TGAC8.**

423 To study the downstream functions of these phosphoproteins, we performed molecular and
424 cellular functions analysis in IPA. The enriched functions were mainly in three categories, i.e.,
425 cell viability, protein quality control, and metabolism (Figure 1F and File 2: Sheet5). The
426 functions of cellular assembly and organization, cellular function and maintenance, and cell

427 death and survival were ranked as the top three terms, indicating the important role of the
428 reprogrammed phosphoproteome in improving cell viability in response to the chronic stress of
429 the overexpression of AC8 in the mouse heart.

430

431 **3. Integrative analyses of transcriptome, proteome and phosphoproteome.**

432 We next integrated changes in PTM (phosphorylation) in TGAC8 vs. WT with genotypic
433 differences in protein translation and in transcription. The circos plot (Figure 3A) illustrates the
434 genotypic differences (TGAC8 vs. WT) in **molecules** identified across the transcriptome,
435 proteome, and phosphoproteome. In addition, the correlation scatter plots (Figure 3B)
436 demonstrated a moderate level of correlation of genotypic differences of molecular changes
437 within phosphoproteome and transcriptome, and a somewhat stronger correlation between
438 genotypic differences of molecular changes within phosphoproteome and proteome (Figure 3C).
439 Concordant and discordant enrichments of canonical pathways differed by genotype among the
440 three omics are shown in Figure 3D. A comparison of genotypic differences within the three
441 omics highlights the importance of protein phosphorylation, and the phosphorylation was
442 **coordinated with and supplemental to** transcription and translation.

443 Because kinases and phosphatases are the key regulators of phosphorylation, and
444 phosphorylation of transcription factors (TFs) are the primary determinant of their activities in
445 transcription, we compared genotypic differences in kinases, phosphatases and TFs within the
446 phosphoproteome and proteome with our previously published genotypic differences in the
447 TGAC8 vs. WT transcriptome[10] (Figure 3E). We identified 196 kinases, 71 phosphatases and
448 191 TFs in the present phosphoproteome (Figure 3F). The protein phosphorylation status of
449 about one half of these molecules differed significantly (p-value < 0.05) by genotype (Figure
450 3G), and the protein phosphorylation status of majority of these molecules was increased (Figure
451 3H-3J). The genotypic differences in the transcription (mRNA expression obtained from RNA-
452 seq) and translation (protein expression obtained from mass spectrometry) of these molecules,
453 however, differed from those in the phosphoproteome (Figure 3E). Because there were more
454 molecules that were unchanged or reduced in the TGAC8 vs. WT transcriptome or proteome
455 than in the phosphoproteome, it is clear that the changes in protein phosphorylation are of utmost
456 importance in the coordination of transcription, translation and PTM, that underlie the adaptive
457 response of the TGAC8 LV to the marked, chronic increase stress of its intrinsically activated
458 AC-cAMP-PKA-Ca^{2+} signaling. Thus, by utilizing multiple bioinformatic analysis methods, we
459 not only dissected the reprogrammed phosphoproteome and deduced its functions in the TGAC8
460 mouse LV, but also profiled the coordination of phosphoproteome, transcriptome and proteome.

461 **3.1. Implications of coordinated changes in protein phosphorylation and transcription in**
462 **TGAC8 vs. WT.**

463 The most likely type of coordination between protein phosphorylation and transcription is related
464 to phosphorylation states of TFs which is determined by kinases and phosphatases activities.
465 Analysis of the remodeled LV transcriptome of TGAC8 in Gene Ontology (GO) analysis using
466 DAVID online software discovered that enrichments of numerous phosphorylation and
467 dephosphorylation related biological processes and molecular functions significantly differed by
468 genotype (Figure 4A), and that the coordinated expression of numerous kinases and
469 phosphatases also differed by genotype (Figure 4B-4C and File 8). Because expression levels of
470 kinases and phosphatases do not denote their activation states, we utilized IPA to predict the
471 genotypic differences in activation states of upstream kinase and phosphatase (regulators of the
472 transcriptome). Intriguingly, 60 kinases were predicted to be upstream regulators of the
473 remodeled LV transcriptome of TGAC8, and the majority of these kinases were predicted to be
474 activated in TGAC8 vs. WT (Figure 4D and File 9). In contrast, much fewer phosphatases were
475 predicted between TGAC8 and WT, and most of these were predicted to be inhibited (Figure 4E
476 and File 9). Thus, the differential genotypic enrichment of phosphorylation status and predicted
477 activation of kinases and phosphatases identified in our post hoc analysis of our previously
478 reported TGAC8 vs. WT transcriptome[10] are linked to the differential genotypic reprogramming
479 of the phosphoproteome discovered in the present study.

480 We utilized IPA to predict the activation states of upstream transcription regulators on the basis
481 of the remodeled LV transcriptomes and proteomes, and then determined their expression levels
482 in transcriptome, proteome and phosphoproteome (Figure 4F). Because TFs are the main
483 regulators of transcription, and because phosphorylation of TFs usually regulates their
484 activities[29-31], we focused our subsequent analysis on functions of those TFs that were
485 differentially phosphorylated in TGAC8 vs. WT. To confirm the hypothesis that the TGAC8
486 might exert transcriptional control by TFs phosphorylation, we retrieved all TFs identified in our
487 previous transcriptome and proteome[10] and mapped them to the current phosphoproteome in
488 order to determine their genotypic differences in phosphorylation status. Of the 191 TFs also
489 identified in this phosphoproteome, 92 TFs differed significantly by genotype in phosphorylation
490 status (p-value < 0.05). In agreement with the general upregulated transcription in TGAC8 LV[10],
491 nearly all of the TFs that differed by genotype had increased phosphorylation level (Figure 4G
492 and File 3). The only exception was purine rich element binding protein G (Purg), known to be
493 hyper-phosphorylated in solid tumors[32].

494 We conducted Kyoto Encyclopedia of Genes and Genomes (KEGG) pathway analysis to further
495 probe the predicted facts of TFs that were generally hyper-phosphorylated in TGAC8 vs. WT.
496 Numerous immunity related pathways, cancer related pathways, and metabolism related
497 pathways were enriched (Figure 4H and File 4). We then utilized IPA for in-depth analysis.
498 Numerous metabolic canonical pathways (glucocorticoid receptor signaling and PPAR
499 signaling), a cancer related canonical pathway (regulation of epithelial-mesenchymal transition
500 pathway), and immunity related canonical pathways (role of JAK1, JAK2 and TYK2 in
501 interferon signaling, IL-9 signaling, JAK/Stat signaling, etc.) were enriched (Figure 4I and File

502 5: Sheet 1). Intriguingly, the sumoylation pathway was markedly inhibited. Because both
503 sumoylation and phosphorylation are important PTMs in transcriptional regulation[33,34], it is
504 possible that the upregulated protein phosphorylation and inhibited protein sumoylation pathway
505 in TFs coordinately activate transcription and improve immunity in the TGAC8 LV. In addition,
506 cell viability and metabolism in molecular and cellular functions were enriched in TGAC8 vs.
507 WT (Figure 4J and File 5: Sheet 2), consistent with enrichments of aforementioned KEGG
508 pathways and IPA canonical pathways (Figure 4H and 4I).

509 Taken together, we have discovered the existence of substantial crosstalk between protein
510 phosphorylation and transcription in the TGAC8 LV: phosphorylation of TFs reprograms
511 immunity and metabolism related pathways and functions in the TGAC8 LV, likely serving to
512 maintain cell survival in response to the chronic stress of marked AC8 overexpression.

513 **3.2. Coordinated changes in protein expression and phosphorylation of the remodeled**
514 **proteome and phosphoproteome of TGAC8.**

515 Having discovered the coordinated changes in the remodeled TGAC8 transcriptome and
516 phosphoproteome (Figure 4A-4E), we next sought to discover the extent to which changes in the
517 remodeled phosphoproteome of the TGAC8 LV were coordinated with changes in its remodeled
518 proteome. Numerous biological processes and molecular functions that were related to
519 phosphorylation and dephosphorylation were enriched in the remodeled TGAC8 LV proteome
520 (Figure 5A), as were numerous kinases and phosphatases (Figure 5B-5C and File 10). Twenty-
521 nine kinases that differed by genotype were predicted to be upstream regulators of the proteome,
522 and most of these were predicted to be activated in TGAC8 vs. WT. Fewer phosphatases than
523 kinases that differed by genotype were identified as upstream regulators of the remodeled
524 TGAC8 LV proteome (Figure 5D-5E and File 11).

525 One strategy adopted to probe deeper into the coordinated changes in the proteome and
526 phosphoproteome of the TGAC8 LV was to normalize the phosphoproteome to the total
527 proteome (in other words, to divide the phosphorylation expression by protein expression) (File
528 1: sheet4). Of the 3927 phosphoproteins identified in our mouse LV samples, 2164 were
529 identified in both the proteome and phosphoproteome, and these were focused for subsequent
530 analyses. After normalization, WT and TGAC8 samples manifested clear genotypic differences
531 in PCA analysis (Figure 5G), and phosphorylation status of numerous proteins normalized to the
532 protein expression level still differed by genotype without cutoff (Figure 5H) and with cutoff (-
533 log(p-value) > 1.3 and absolute(log2(TG/WT)) ≥ 0.4) (Figure 5I). Even after normalizing the
534 phosphorylation level to the protein expression level, the enrichments of canonical pathways in
535 TGAC8 were quite consistent with those of unnormalized phosphoproteome (Figure 5J and File
536 6). Cardiac hypertrophy signaling (enhanced) and cardiac hypertrophy signaling took the top two
537 places, emphasizing the important role of phosphorylation in the regulation of cardiac functions
538 in response to chronic stress when coordinated with changes in the total proteome.

539 Many important stress-response signaling pathways were enriched from phosphoproteome, e.g.,
540 PKA signaling, ERK/MAPK signaling, insulin receptor signaling, and PI3K/AKT signaling
541 (Figure 6A). Three of these pathways, PI3K/AKT, ERK/MAPK and ubiquitin labeling, were also
542 markedly enriched in our previous analysis on total proteome in TGAC8 LV[10]. By integrating
543 and comparing the enrichments from transcriptome, proteome and phosphoproteome, we were
544 able to identify the three signaling pathways in the TGAC8 LV, PI3K/AKT, ERK/MAPK and
545 ubiquitin labeling, that were regulated concordantly in transcription, translation, and PTM
546 (phosphorylation) (Figure 6B). WB validated activation of PI3K/AKT signaling pathway in
547 TGAC8, reproducing the results of our prior study using different antibodies (Figure 6C-6D and
548 Supplementary 3A (more significant)). We also demonstrated in that study that ERK/MAPK
549 signaling was also activated in TGAC8 vs. WT (Supplementary 3B-3C). Activation of
550 PI3K/AKT and ERK/MAPK signaling is crucial for enhanced protein quality control (the
551 increase in protein synthesis and degradation) in the TGAC8 LV[10] (Supplementary 3D- 3G).
552 Although protein ubiquitination, an important process in protein degradation, was enriched in
553 TGAC8 LV within IPA analysis, its activity could not be predicted on the basis of present
554 knowledge base of IPA. Its WB analysis, however, indicated that ubiquitination is indeed
555 increased in TGAC8 vs. WT (Figure 6E).

556 We next sought to identify which molecules linked to PI3K/AKT signaling (one of the most
557 important pathways in this mouse model) differed in TGAC8 vs. WT. Among the significantly
558 changed upstream molecules, the majority were upregulated. AKT, a central molecule in the
559 pathway, was also increased in proteome and phosphoproteome (Figure 6F). By searching and
560 mapping the substrates of AKT, we unraveled that the phosphorylation levels of AKT peptide
561 substrates were mostly elevated in TGAC8 vs. WT (Figure 6G). Therefore, the downstream
562 effects and functions of AKT signaling were activated in TGAC8 LV: (1) upregulating GSK3 to
563 improve energy metabolism; (2) activating mTOR pathway to increase protein synthesis and cell
564 growth; (3) promoting NF-κB mediated transcription; (4) upregulating BAD and eNOS only at
565 phosphorylation level to enhance cell survival and cardiovascular functions. In summary, to
566 adapt the heart to stress for improved survival, the TGAC8 reprogram the cardiac LV
567 phosphoproteome to a large degree.

568

569 **4. Discordant regulation of the phosphoproteome and proteome in TGAC8 LV.**

570 Among the 443 proteins that differed by genotype in both protein phosphorylation and protein
571 expression levels, 33 were changed discordantly at the two levels (in opposite directions, i.e.,
572 upregulated in proteome but downregulated in phosphoproteome, or vice versa) (Figure 7A and
573 File 7: Sheet 1). We uploaded the 33 discordant proteins into STRING online software for
574 functional analyses. The GO_CC (Cellular Component) analysis resulted in many
575 **mitochondrial components**, indicating the involvement of phosphorylated proteins in
576 mitochondria (Figure 7B and File 7: Sheet 2). Reactome pathway analysis showed that in

577 addition to mitochondria, metabolic pathways were enriched significantly in TGAC8 (Figure 7C
578 and File 7: Sheet 3). Mitochondria are the hub of metabolism and multiple metabolic processes
579 are executed in mitochondria. Consistently, both metabolism and mitochondria related processes
580 were ranked the top processes in GO_BP (Biological Process) analysis (Figure 7D and File 7:
581 Sheet 4). Therefore, the discordant part between total proteome and phosphoproteome indicated
582 that the phosphorylation plays a critical role in the regulation of mitochondria and metabolism in
583 the TGAC8, distinct from its role in regulation at the translational level.

584

585 **5. Deduced schematic of coordination of phosphoproteome with transcriptome and**
586 **proteome in TGAC8 mouse LV.**

587 A deduced schematic integration of the remodeled phosphoproteome, proteome and
588 transcriptome of the TGAC8 LV is shown in Figure 8. The TGAC8 mouse initially induces a
589 PKA dependent phosphorylation via AC8-cAMP-PKA axis. Many cytoplasmic proteins
590 including TFs are thus phosphorylated and then transported into the nucleus where TFs
591 recognize and bind to the promoters to activate the transcription of more regulatory factors,
592 including kinases, phosphatases, and TFs. The activation states of these factors are changed upon
593 phosphorylated in cytosol, thereby activating additional kinases-controlled phosphorylation
594 cascades and reprogramming the cardiac phosphoproteome comprehensively.

595

596 **Discussion**

597 Our prior study[10] investigated the adaptive mechanisms that emerge in the TGAC8 heart to
598 marked chronic stress of increased AC8-cAMP-PKA-Ca^{2+} signaling. In that study, a large
599 number of proteins differed in TGAC8 vs. WT. The TGAC8 induced a chronic cardiac exercise
600 phenotype in the heart, i.e., an increase in heart rate and contractility. These functional changes
601 were accompanied by an increased cardiac biomass and energy demand. Multiple signaling
602 pathways, related to nutrient sensing, energy production, cardiac cellular stress, cardiac stress
603 response, growth factor signaling, and cell proliferation, were identified as downstream
604 mediating the effect of the activated AC8-cAMP-PKA-Ca^{2+} signaling in the TGAC8 LV.

605 Our goals here were to determine which proteins in TGAC8 LV differed in expression and
606 phosphorylation status compared to WT, and which kinases/phosphatases play roles in these
607 altered phosphorylation statuses in the TGAC8. By the utilization of TMT-labeling MS, we
608 obtained 12963 phosphopeptides and 3646 phosphoproteins, and observed the general
609 upregulation of phosphorylation. We observed the enrichments of phosphorylation, upregulated
610 expression of kinases, and predicted activation of upstream kinases. We made use of
611 phosphoproteome complementary to transcriptome and proteome to expand our understanding of
612 the regulatory mechanism how the TGAC8 adapts to chronic stress of activated AC8-cAMP-
613 PKA-Ca^{2+} signaling. This approach enabled us to appreciate how changes in the transcription,

614 translation and PTM of proteins in the TGAC8 LV may singly or coordinately enable the
615 TGAC8 to endure the chronic AC8-induced stress (Figure 8).

616 First, the TGAC8 induced a PKA dependent phosphorylation via the AC8-cAMP-PKA axis
617 (typical substrate motif of PKA dependent phosphorylation). Most of previous studies only
618 focused on PKA phosphorylated targets as downstream effects of activated AC8. For example,
619 AC8 induced cAMP activates PKA to increase the phosphorylation of many key proteins in
620 cardiovascular system, e.g., ryanodine-receptor-type 2 (RyR2), L-type Ca^{2+} channels (LTCC),
621 phospholamban (PLN or PLB), etc[10]. In this research, we identified 29 phosphosites on RyR2, 15
622 phosphosites on LTCC alpha 1 and beta 2, and 2 phosphosites (S16 and T17) on PLN. SERCA2
623 and the majority of them were increased in phosphorylation statuses in the TGAC8 LV (File 1:
624 Sheet 1). It is worth noting that PLN is phosphorylated on S16 by PKA whereas on T17 by Ca^{2+}-
625 calmodulin-dependent protein kinase (CaMKII)[35].

626 After the activation of phosphorylation cascade, many cytoplasmic proteins including TFs were
627 thus phosphorylated and then transported into the nucleus where TFs recognize and bind to the
628 promoters to activate transcription. For example, Figure 4 F and 4G showed that many
629 transcriptional regulators were phosphorylated in TGAC8 vs. WT. The phosphorylation of
630 STAT1[36,37], STAT3[37], HTT[38] and CREB1[39] is associated with the activation of their
631 transcriptional activities. The elevated TFs phosphorylation and possibly activated transcription
632 were consistent with the general increase in transcriptome[10]. The hyper-phosphorylated TFs
633 might contribute to the improved immunity, metabolism and cell viability in TGAC8 (Figure 4H-
634 4I). For example, STAT family proteins are transcription activators, and their phosphorylation is
635 involved in inflammation and immune response[40,41]. The present study identified increased
636 phosphorylation levels in S727 on STAT1 and S726/S727 on STAT3 (File 1: Sheet 1), in line
637 with our previous report which identified hyper-phosphorylation of components within
638 inflammation and immune response signaling pathways such as JAK/STAT and JNK
639 pathways[10].

640 Upon the activation of RNA transcription, numerous molecules, including kinases, phosphatases,
641 and TFs, were transcribed more in TGAC8 than WT, thereby, activating other kinases-controlled
642 phosphorylation cascades in addition to PKA. The additional kinases and phosphorylation
643 cascades could also be directly activated by the overexpression of AC8 in another manner to be
644 determined. In this study, with the three datasets, IPA predicted many other kinase-substrate
645 reactions in addition to PKA. PDPK1, PAK1 and PTK2B were the three most consistent kinases.
646 In the context of the overexpression of AC8, these three kinases could be activated to
647 phosphorylate multiple proteins to activate PKA pathway (positive feedback) and MAPK/ERK
648 pathway (also known as Ras-Raf-MEK-ERK pathway) to maintain heart health (Figure 1E and
649 Supplementary Figure 2). Previously, we showed their WB results that MAPK/ERK pathway
650 were activated due to increased protein expression of p21 Ras and the elevated phosphorylation
651 levels of c-Raf, MEK1/2 and ERK1/2 as well as their increased ratios of phosphorylation to
652 protein expression[10]. In the present study, S233 and S621/S641 on Isoform 2 of RAF proto-

653 oncogene serine/threonine-protein kinase were hyper-phosphorylated in TGAC8 (File 1: Sheet
654 1). Importantly, the multifunctional molecule, GSK3B, was the downstream of PDPK1 and
655 PTK2B in the integrated regulation network. GSK3B is involved in metabolism and cardiac
656 hypertrophy[42,43]. Interestingly, AC8 is required for glucose homeostasis and hypothalamic
657 adaptation to high-fat diet[44]. The phosphorylation of GSK3B is also a critical mediator in
658 convergence of cardioprotection signaling[27,28]. We previously detected the increase in the protein
659 expression of GSK3B[10] and here identified the hyper-phosphorylated S9 on GSK3B (File 1:
660 Sheet 1). The bioinformatic analysis strategy here revealed a larger kinase-substrate network
661 important in the remodeling of the TGAC8 heart. We plan to validate these kinase-substrate
662 reactions in more follow-up studies and provide the reliable mechanism in cardiovascular
663 research.

664 Taken together, the TGAC8 upregulates phosphorylation to reprogram the heart. Based on
665 results in this study combined with our recently published work on TGAC8 LV[10], we generated a
666 comprehensive circuitry (Supplementary Figure 4). Navigating this figure "by the numbers":
667 marked, chronic, cardiac specific overexpression of AC8 (1) chronically increases cAMP (2) and
668 PKA-Ca^{2+} signaling (3), resulting, not only in an incessantly increased cardiac performance, due
669 to elevated heart rate and LV contractility (4), but also activation of growth factor signaling
670 pathways (5), leading to increase in energy demand due to increased transcription and increased
671 amino acid, nucleotide, protein, lipid and lipoprotein synthesis, increased protein quality control,
672 including proteosome activity, autophagy, mitophagy, cytokine signaling and inflammation (6).
673 Chronic high level of AC8 activation elicits numerous stress responses (8) including increased
674 nutrient sensing with increased AMPK signaling (10A), increased ROS scavenging, protection
675 against cell death, and also induction of signaling to minimize the impact of AC-PKA signaling
676 (10B). Shifts in energy production and utilization to deal with the marked energy demands of the
677 TGAC8 heart (10, 12) include: enhancement of glucose metabolism is pronounced (11, 13),
678 whilst utilization of fatty acids to produce energy is reduced (11) but an increase in glucose
679 catabolism (10, 11) is accompanied by an increased anabolism (12), supported by increased
680 aerobic glycolysis (11,13); increased utilization of the pentose phosphate shunt (5, 13) supports
681 increased amino acid, nucleotide, protein and lipoprotein synthesis induced by growth factor
682 signaling (5), resulting in an increase in LV biomass (14). This adaptive profile balances energy
683 requirements necessary for an incessant marked increase in cardiac performance (4), for
684 increased RNA transcription, protein translation and quality control required for cardiac growth
685 (14), and for other biological processes within the LV myocardium (6). This pattern of consilient
686 adaptations (6-15) sustains an incessant increase in cardiac performance while conferring cardio-
687 protection to the TGAC8 heart.

688 **Open questions and limitations**

689 In addition to the fascinating adaptive mechanisms in the TGAC8 LV discussed above, the
690 present research also raised some interesting open-mind questions, such as cardiac hypertrophy
691 signaling and sumoylation pathway enriched here.

692 Although the cardiac β-AR signaling is desensitized in many pathological conditions, like aging,
693 so as to despair the cardiovascular system functions, cAMP bioavailability could maintain
694 cardiac functions in the aged heart. Based on this, the overexpression of AC8 in heart was
695 regarded as a potential therapeutic way to increase the bioavailability of cardiac cAMP
696 independent of β-AR stimulation to improve cardiac functions[7]. Unexpectedly, the cardiac-
697 specific chronic activation of the cAMP pathway (overexpressing β1- AR, β2-AR, Gas, PKA,
698 PP1 inhibitor-1 (I-1), etc.) that enhances cardiac functions in young animals induces progressive
699 cardiomyopathy and premature death during aging[45]. Consistently, in the present research,
700 although the enriched cardiac hypertrophy signaling (enhanced) was not accompanied with the
701 markable hypertrophy phenotype in young male TGAC8 mice, it indicated a cardiac remodeling
702 that could lead to hypertrophy if accompanied with additional stresses, like aging. This
703 assumption was supported by another research on the TGAC8 mouse which reported early
704 alterations of myocardial structure, i.e., cardiomyocyte hypertrophy and endocardial fibrosis, in
705 twelve-month old TGAC8 mice compared with their WT littermates[46]. Therefore, our established
706 bioinformatic analysis strategy is a novel paradigm in **predicting** progressive cardiomyopathy
707 and premature death using early reprograming of omics in young age. More importantly, the
708 mechanisms discovered here in the young adult TGAC8 mice could be utilized in maintaining
709 cardiac health in older TGAC8 mice.

710 Interestingly, more and more PTMs have been discovered nowadays and they often occur at the
711 same time or on the same protein to carry important biological processes coordinately[47,48]. For
712 example, in rat hearts subjected to ischemia, lysine acetylation interferes with activities of
713 protein kinases to increase proximal dephosphorylation, which is involved in the regulation of
714 cell survival or death[49]. In the present research, sumoylation pathway was inhibited along with
715 the upregulated phosphorylation (Figure 4I), indicating the cross-talk between these two PTMs
716 in the mouse heart. In human cell-lines, the switch from phosphorylation to sumoylation could
717 repress the Raf/MEK/ERK signaling to improve the immunity, resulting in the declined infection
718 of influenza A virus[50]. In human HEK293 cells, the coordinated phosphorylation and
719 sumoylation can also control MEF2 transcriptional activity[51]. However, the competition of
720 phosphorylation and sumoylation in cardiomyocytes was unclear. In this research, we observed
721 the upregulated phosphorylation and inhibited sumoylation pathway enriched from TFs in the
722 TGAC8 mouse LV. The regulated PTMs were speculated to be involved in the increased
723 transcription and improved immunity. To validate the effect on sumoylation by elevated
724 phosphorylation in our next studies, we could perform WB with the antibody against pan-
725 sumoylation to detect the general sumoylation change in the TGAC8 LV. In addition, we could
726 detect the sumoylation changes after mimicry upregulation or downregulation of phosphorylation
727 using activators or inhibitors in primary cardiomyocytes to prove the interplay between
728 phosphorylation and sumoylation in cardiomyocytes.

729 **Summary**

730 The reprogrammed phosphoproteome activated stress response signaling pathways to defend
731 against cardiac stress in young mice, improve cell viability and suppress cell death. On one hand,
732 the reprogramed phosphoproteome enhances transcription to improve the immunity and
733 metabolism; on the other hand, it coordinates with the proteome to improve mitochondrial
734 functions and metabolism. Finally, although we revealed the coordination of regulation at
735 different levels, which provides a roadmap to guide the integration of transcription, translation
736 and PTM, our results set the stage for additional studies in this remarkable TGAC8 model: What
737 kinases are specifically involved in the PTM identified here? How are these phosphorylated
738 proteins specifically distributed in subcellular locations? The present study focuses on a
739 comprehensive in silico analysis of functionally coherent and data-driven transcription,
740 translation, and post-translation patterns that were well translated in the contribution to AC8-
741 overexpression cardiac outcomes, while further investigation is warranted to see whether the hub
742 pathway/function predictions via gene sets, phosphopeptides, and phosphoproteins could be used
743 as biomarkers or impact the diagnostic specificity for transgenic AC8 cardiac health and
744 pathology.

745

746 **Acknowledgements**

747 We thank all members in Laboratory of Cardiovascular Science, National Institute on Aging, National
748 Institutes of Health, for technical assistance and discussion. This work utilized the computational
749 resources of the NIH HPC Biowulf cluster (http://hpc.nih.gov).

750

751 **Sources of Funding**

752 Intramural Research Program at National Institute on Aging, National Institutes of Health.

753

754 **Disclosures**

755 None.

756

757 **References**

758 1 Halls, M. L. & Cooper, D. M. F. Adenylyl cyclase signalling complexes - Pharmacological
759 challenges and opportunities. *Pharmacol Ther* **172**, 171-180 (2017).
760 https://doi.org:10.1016/j.pharmthera.2017.01.001
761 2 Dessauer, C. W. *et al.* International Union of Basic and Clinical Pharmacology. CI. Structures and
762 Small Molecule Modulators of Mammalian Adenylyl Cyclases. *Pharmacological reviews* **69**, 93-
763 139 (2017). https://doi.org:10.1124/pr.116.013078
764 3 Willoughby, D. *et al.* A key phosphorylation site in AC8 mediates regulation of Ca(2+)-dependent
765 cAMP dynamics by an AC8-AKAP79-PKA signalling complex. *J Cell Sci* **125**, 5850-5859 (2012).
766 https://doi.org:10.1242/jcs.111427

767 4 Sadana, R. & Dessauer, C. W. Physiological roles for G protein-regulated adenylyl cyclase
768 isoforms: insights from knockout and overexpression studies. *Neuro-Signals* **17**, 5-22 (2009).
769 https://doi.org:10.1159/000166277
770 5 Georget, M. *et al.* Augmentation of cardiac contractility with no change in L-type Ca2+ current in
771 transgenic mice with a cardiac-directed expression of the human adenylyl cyclase type 8 (AC8).
772 *Faseb j* **16**, 1636-1638 (2002). https://doi.org:10.1096/fj.02-0292fje
773 6 Ferguson, G. D. & Storm, D. R. Why calcium-stimulated adenylyl cyclases? *Physiology (Bethesda,*
774 *Md.)* **19**, 271-276 (2004). https://doi.org:10.1152/physiol.00010.2004
775 7 Lipskaia, L. *et al.* Enhanced cardiac function in transgenic mice expressing a Ca(2+)-stimulated
776 adenylyl cyclase. *Circ. Res.* **86**, 795-801 (2000). https://doi.org:10.1161/01.res.86.7.795
777 8 Esposito, G. *et al.* Increased myocardial contractility and enhanced exercise function in
778 transgenic mice overexpressing either adenylyl cyclase 5 or 8. *Basic Res Cardiol* **103**, 22-30
779 (2008). https://doi.org:10.1007/s00395-007-0688-6
780 9 Moen, J. M. *et al.* Overexpression of a Neuronal Type Adenylyl Cyclase (Type 8) in Sinoatrial
781 Node Markedly Impacts Heart Rate and Rhythm. *Front Neurosci* **13**, 615 (2019).
782 https://doi.org:10.3389/fnins.2019.00615
783 10 Tarasov, K. V. *et al.* A remarkable adaptive paradigm of heart performance and protection
784 emerges in response to the constitutive challenge of marked cardiac-specific overexpression of
785 adenylyl cyclase type 8. *eLife* **11**, e80949 (2022). https://doi.org:10.7554/eLife.80949
786 11 Qu, J.-H. *et al.* Proteomic Landscape and Deduced Functions of the Cardiac 14-3-3 Protein
787 Interactome. *Cells* **11**, 3496 (2022). https://doi.org:10.3390/cells11213496
788 12 Consortium, T. U. UniProt: a worldwide hub of protein knowledge. *Nucleic Acids Res.* **47**, D506-
789 D515 (2018). https://doi.org:10.1093/nar/gky1049
790 13 Crooks, G. E., Hon, G., Chandonia, J. M. & Brenner, S. E. WebLogo: a sequence logo generator.
791 *Genome research* **14**, 1188-1190 (2004). https://doi.org:10.1101/gr.849004
792 14 Colaert, N., Helsens, K., Martens, L., Vandekerckhove, J. & Gevaert, K. Improved visualization of
793 protein consensus sequences by iceLogo. *Nat Methods* **6**, 786-787 (2009).
794 https://doi.org:10.1038/nmeth1109-786
795 15 Mitaku, S., Hirokawa, T. & Tsuji, T. Amphiphilicity index of polar amino acids as an aid in the
796 characterization of amino acid preference at membrane-water interfaces. *Bioinformatics* **18**,
797 608-616 (2002). https://doi.org:10.1093/bioinformatics/18.4.608
798 16 Takahashi, S. & Mendelsohn, M. E. Synergistic activation of endothelial nitric-oxide synthase
799 (eNOS) by HSP90 and Akt: calcium-independent eNOS activation involves formation of an
800 HSP90-Akt-CaM-bound eNOS complex. *The Journal of biological chemistry* **278**, 30821-30827
801 (2003). https://doi.org:10.1074/jbc.M304471200
802 17 Lim, G., Venetucci, L., Eisner, D. A. & Casadei, B. Does nitric oxide modulate cardiac ryanodine
803 receptor function? Implications for excitation-contraction coupling. *Cardiovasc Res* **77**, 256-264
804 (2008). https://doi.org:10.1093/cvr/cvm012
805 18 Meissner, G. in *Structure and Function of Calcium Release Channels Current Topics in*
806 *Membranes* 91-113 (2010).
807 19 Hunzicker-Dunn, M. E. *et al.* PKA and GAB2 play central roles in the FSH signaling pathway to
808 PI3K and AKT in ovarian granulosa cells. *Proceedings of the National Academy of Sciences of the*
809 *United States of America* **109**, E2979-2988 (2012). https://doi.org:10.1073/pnas.1205661109
810 20 Bellis, A. *et al.* Cross-talk between PKA and Akt protects endothelial cells from apoptosis in the
811 late ischemic preconditioning. *Arterioscler Thromb Vasc Biol* **29**, 1207-1212 (2009).
812 https://doi.org:10.1161/atvbaha.109.184135

21 Desai, S., Pillai, P., Win-Piazza, H. & Acevedo-Duncan, M. PKC-iota promotes glioblastoma cell survival by phosphorylating and inhibiting BAD through a phosphatidylinositol 3-kinase pathway. *Biochim Biophys Acta* **1813**, 1190-1197 (2011). https://doi.org:10.1016/j.bbamcr.2011.03.007

22 Li, Y. *et al.* microRNA-378 promotes autophagy and inhibits apoptosis in skeletal muscle. *Proceedings of the National Academy of Sciences of the United States of America* **115**, E10849-e10858 (2018). https://doi.org:10.1073/pnas.1803377115

23 Chen, X. *et al.* PDK1 regulates platelet activation and arterial thrombosis. *Blood* **121**, 3718-3726 (2013). https://doi.org:10.1182/blood-2012-10-461897

24 Ericson, K. *et al.* Genetic inactivation of AKT1, AKT2, and PDPK1 in human colorectal cancer cells clarifies their roles in tumor growth regulation. *Proceedings of the National Academy of Sciences of the United States of America* **107**, 2598-2603 (2010). https://doi.org:10.1073/pnas.0914018107

25 Hartigan, J. A., Xiong, W. C. & Johnson, G. V. Glycogen synthase kinase 3beta is tyrosine phosphorylated by PYK2. *Biochemical and biophysical research communications* **284**, 485-489 (2001). https://doi.org:10.1006/bbrc.2001.4986

26 Tsai, C. C. *et al.* Glycogen synthase kinase-3beta facilitates IFN-gamma-induced STAT1 activation by regulating Src homology-2 domain-containing phosphatase 2. *J Immunol* **183**, 856-864 (2009). https://doi.org:10.4049/jimmunol.0804033

27 Juhaszova, M. *et al.* Glycogen synthase kinase-3beta mediates convergence of protection signaling to inhibit the mitochondrial permeability transition pore. *The Journal of clinical investigation* **113**, 1535-1549 (2004). https://doi.org:10.1172/JCI19906

28 Juhaszova, M. *et al.* Role of glycogen synthase kinase-3beta in cardioprotection. *Circ. Res.* **104**, 1240-1252 (2009). https://doi.org:10.1161/CIRCRESAHA.109.197996

29 Bohmann, D. Transcription factor phosphorylation: a link between signal transduction and the regulation of gene expression. *Cancer cells (Cold Spring Harbor, N.Y. : 1989)* **2**, 337-344 (1990).

30 Weigel, N. L. & Moore, N. L. Steroid receptor phosphorylation: a key modulator of multiple receptor functions. *Molecular endocrinology (Baltimore, Md.)* **21**, 2311-2319 (2007). https://doi.org:10.1210/me.2007-0101

31 Mayr, B. & Montminy, M. Transcriptional regulation by the phosphorylation-dependent factor CREB. *Nature reviews. Molecular cell biology* **2**, 599-609 (2001). https://doi.org:10.1038/35085068

32 Zanivan, S. *et al.* Solid tumor proteome and phosphoproteome analysis by high resolution mass spectrometry. *J Proteome Res* **7**, 5314-5326 (2008). https://doi.org:10.1021/pr800599n

33 Tomanov, K. *et al.* Sumoylation and phosphorylation: hidden and overt links. *Journal of Experimental Botany* **69**, 4583-4590 (2018). https://doi.org:10.1093/jxb/ery167

34 Khan, M. *et al.* Interplay between phosphorylation and SUMOylation events determines CESTA protein fate in brassinosteroid signalling. *Nat Commun* **5**, 4687 (2014). https://doi.org:10.1038/ncomms5687

35 Wegener, A. D., Simmerman, H. K., Lindemann, J. P. & Jones, L. R. Phospholamban phosphorylation in intact ventricles. Phosphorylation of serine 16 and threonine 17 in response to beta-adrenergic stimulation. *The Journal of biological chemistry* **264**, 11468-11474 (1989).

36 Pilz, A. *et al.* Phosphorylation of the Stat1 transactivating domain is required for the response to type I interferons. *EMBO reports* **4**, 368-373 (2003). https://doi.org:10.1038/sj.embor.embor802

37 Wen, Z., Zhong, Z. & Darnell, J. E., Jr. Maximal activation of transcription by Stat1 and Stat3 requires both tyrosine and serine phosphorylation. *Cell* **82**, 241-250 (1995). https://doi.org:10.1016/0092-8674(95)90311-9

859 38 Kumar, A., Vaish, M. & Ratan, R. R. Transcriptional dysregulation in Huntington's disease: a
860 failure of adaptive transcriptional homeostasis. *Drug Discov. Today* **19**, 956-962 (2014).
861 https://doi.org:10.1016/j.drudis.2014.03.016
862 39 Wang, H., Xu, J., Lazarovici, P., Quirion, R. & Zheng, W. cAMP Response Element-Binding Protein
863 (CREB): A Possible Signaling Molecule Link in the Pathophysiology of Schizophrenia. *Frontiers in*
864 *molecular neuroscience* **11**, 255-255 (2018). https://doi.org:10.3389/fnmol.2018.00255
865 40 Seif, F. *et al.* The role of JAK-STAT signaling pathway and its regulators in the fate of T helper
866 cells. *Cell Communication and Signaling* **15**, 23 (2017). https://doi.org:10.1186/s12964-017-
867 0177-y
868 41 Decker, T. & Kovarik, P. Serine phosphorylation of STATs. *Oncogene* **19**, 2628-2637 (2000).
869 https://doi.org:10.1038/sj.onc.1203481
870 42 Beurel, E., Grieco, S. F. & Jope, R. S. Glycogen synthase kinase-3 (GSK3): regulation, actions, and
871 diseases. *Pharmacol Ther* **148**, 114-131 (2015).
872 https://doi.org:10.1016/j.pharmthera.2014.11.016
873 43 Lal, H., Ahmad, F., Woodgett, J. & Force, T. The GSK-3 family as therapeutic target for myocardial
874 diseases. *Circ Res* **116**, 138-149 (2015). https://doi.org:10.1161/circresaha.116.303613
875 44 Raoux, M. *et al.* Multilevel control of glucose homeostasis by adenylyl cyclase 8. *Diabetologia*
876 **58**, 749-757 (2015). https://doi.org:10.1007/s00125-014-3445-z
877 45 El-Armouche, A. & Eschenhagen, T. Beta-adrenergic stimulation and myocardial function in the
878 failing heart. *Heart failure reviews* **14**, 225-241 (2009). https://doi.org:10.1007/s10741-008-
879 9132-8
880 46 Mougenot, N. *et al.* Cardiac adenylyl cyclase overexpression precipitates and aggravates age-
881 related myocardial dysfunction. *Cardiovascular research* **115**, 1778-1790 (2019).
882 https://doi.org:10.1093/cvr/cvy306
883 47 Beltrao, P., Bork, P., Krogan, N. J. & van Noort, V. Evolution and functional cross-talk of protein
884 post-translational modifications. *Molecular systems biology* **9**, 714 (2013).
885 https://doi.org:10.1002/msb.201304521
886 48 Venne, A. S., Kollipara, L. & Zahedi, R. P. The next level of complexity: crosstalk of
887 posttranslational modifications. *Proteomics* **14**, 513-524 (2014).
888 https://doi.org:10.1002/pmic.201300344
889 49 Parker, B. L. *et al.* Structural basis for phosphorylation and lysine acetylation cross-talk in a
890 kinase motif associated with myocardial ischemia and cardioprotection. *The Journal of biological*
891 *chemistry* **289**, 25890-25906 (2014). https://doi.org:10.1074/jbc.M114.556035
892 50 Wang, C. *et al.* HA Triggers the Switch from MEK1 SUMOylation to Phosphorylation of the ERK
893 Pathway in Influenza A Virus-Infected Cells and Facilitates Its Infection. *Frontiers in cellular and*
894 *infection microbiology* **7**, 27 (2017). https://doi.org:10.3389/fcimb.2017.00027
895 51 Grégoire, S. *et al.* Control of MEF2 transcriptional activity by coordinated phosphorylation and
896 sumoylation. *The Journal of biological chemistry* **281**, 4423-4433 (2006).
897 https://doi.org:10.1074/jbc.M509471200

898

899

900

901

902

903 **Figure Legends**

904 **Figure 1. TGAC8 reprograms the LV phosphorylation state. A**. PCA plot of phosphoproteome in
905 TGAC8 vs. WT LVs. **B**. Heatmap of scaled expressions of phosphorylated proteins. **C**. Volcano plot of
906 phosphoproteome. Red dots represent upregulated phosphoproteins with -log10(p-value) > 1.3 and
907 log2(fold change) ≥ 0.4; blue dots represent downregulated phosphoproteins with -log10(p-value) > 1.3
908 and log2(fold change) ≤ -0.4; grey dots represent nonsignificantly regulated phosphoproteins with -
909 log10(p-value) ≤ 1.3 or absolute(log2(fold change)) < 0.4. **D**. Top 21 canonical pathways enriched from
910 phosphoproteome. Orange and blue bars represent activated and inhibited pathways respectively. The
911 darker the color is, the greater the absolute(z-score) is, and the more significantly enriched the pathway is.
912 **E**. Regulatory pathway from upstream kinases. Three dots in the center represent the predicted upstream
913 kinases. Surrounding dots represent identified phosphoproteins differentially regulated in
914 phosphoproteome. Terms on the bottom represent canonical pathways in which the phosphoproteins are
915 involved. Meanings of colors refer to the box of prediction legend besides the graph. **F**. Enriched
916 molecular and cellular functions from the phosphoproteome. They are related to three categories,
917 including cell viability, protein quality control, and metabolism.

918

919 **Figure 2. Characteristics of upregulated phosphopeptides. A**. Composition of phosphosites that reside
920 on the upregulated phosphopeptides. **B**. Sequence logo diagrams of upregulated phosphopeptides centered
921 on the phosphosites and flanked by 6 amino acids on the N and C termini respectively using WebLogo
922 online software. Colors of amino acids represent different chemical properties. **C**. Western blots of
923 phosphorylation of PKA substrates and their statistics results: RRXS*/T*. Unpaired Student's t test with
924 Welch's correction was used. **D**. Test the amphiphilicity feature of the upregulated phosphopeptides using
925 iceLogo online software and referring to a published work by Mitaku and colleagues in 2002[15].

926

927 **Figure 3. Integrative analysis of transcriptome, proteome and phosphoproteome. A**. Circos plot of
928 gene expression at different levels from transcription, to protein, and to phosphorylation. Bars in each
929 layer of circle represent changes of significantly regulated molecules (q-value or p-value < 0.05) in
930 transcriptome, total proteome, and unnormalized phosphoproteome. Bar height, color and direction
931 represent log2(fold change). Red and upward indicate upregulation, and blue and downward indicate
932 downregulation. **B-C**. Scatter plots of correlation between phosphoproteome and transcriptome (**B**) or
933 total proteome (**C**). **D**. Comparison of canonical pathway enrichments from the transcriptome, total
934 proteome, and phosphoproteome. Enrichment z-scores were calculated in IPA, and were scaled to
935 generate heatmap in R language. **E**. Integrative graph of expression of all phosphoproteins and selected
936 types of molecules. Bar plot on the bottom displays expression of all significantly changed (p-value <
937 0.05) phosphoproteins in unnormalized phosphoproteome. Y-axis denotes log2(fold change), and x-axis
938 denotes each molecule ranked by log2(fold change). Bars were colored by -log10(p-value). Stick plots on
939 the top display kinases, phosphatases and transcription factors (TFs) selected from the bottom bar plot and
940 their changes in transcriptome (RNA), total proteome (pro), and normalized phosphoproteome (norm).
941 From top to bottom: each large block denotes the changes of certain types of molecules (from kinases to
942 phosphatases, to TFs). In each block, the three rows from top to bottom indicate the changes in
943 transcriptome, total proteome, and normalized phosphoproteome. Each stick represents a molecule and

color represents the change: red: (p-value or q-value < 0.05) and log2FC > 0; blue: (p-value or q-value < 0.05) and log2FC < 0; black: (p-value or q-value ≥ 0.05) or log2FC = 0; grey: unidentified in one of the omics. Their locations are matched to those in the bottom bar plot. **F-J**. Pie plots of composition of phosphoproteins in the unnormalized phosphoproteome. Regardless of p-value, numbers of four types of proteins, including kinases, phosphatases, TFs and others, are displayed in **F**. After filtration with cutoff p-value < 0.05, numbers of those types of proteins are displayed in **G**. Extracted from G, numbers of upregulated and downregulated kinases (**H**), phosphatases (**I**) and TFs (**J**) are displayed.

Figure 4. Coordination of phosphoproteome and transcriptome. A. GO term enrichments of biological processes and molecular functions about phosphorylation and dephosphorylation from transcriptome. **B-C**. Changes of kinases (**B**) and phosphatases (**C**) whose q-values are less than 0.05 in transcriptome. **D-E**. States of upstream kinases (**D**) and phosphatases (**E**) predicted based on transcriptome. Z-scores were calculated in IPA. Positive and negative z-scores indicate activated and inhibited states respectively. The larger absolute values of z-score indicate more activated or inhibited states. **F**. Heatmap of predicted upstream transcription regulators (left) and their changes in different omics datasets (right). Left: Fill color represent activation z-scores in transcriptome and total proteome. Red and blue indicate activated and inhibited states respectively. Molecules are ranked by z-scores in transcriptome. Right: Fill color represent changes in transcriptome, total proteome, unnormalized phosphoproteome, and normalized phosphoproteome: orange: (p-value or q-value < 0.05) and log2FC > 0; yellow: (p-value or q-value ⩾ 0.05) and log2FC > 0; green: (p-value or q-value < 0.05) and log2FC < 0; light blue: (p-value or q-value ⩾ 0.05) and log2FC < 0; grey: unidentified in one of the omics. **G**. Changes of differentially regulated TFs with p-value < 0.05 in the unnormalized phosphoproteome. **H**. KEGG pathway enrichments of the differentially regulated TFs. They are in four primary categories: cancer, immunity, metabolism and others. **I**. Top 20 canonical pathways enriched from the phosphoproteome using IPA. The darker the color is, the greater the absolute(z-score) is, and the more significantly enriched the pathway is. **J**. Enriched molecular and cellular functions from the phosphoproteome using IPA. They are in two primary categories: cell viability and metabolism.

Figure 5. Analysis of normalized phosphoproteome. A. GO term enrichments of biological processes and molecular functions about phosphorylation and dephosphorylation from the present proteome. **B-C**. Changes of kinases (**B**) and phosphatases (**C**) whose q-values are less than 0.05 in previous proteome. **D-E**. States of upstream kinases (**D**) and phosphatases (**E**) predicted based on the present proteome. Z-scores were calculated in IPA. Positive and negative z-scores indicate activated and inhibited states respectively. The larger absolute values of z-score indicate more activated or inhibited states. **F**. Venn plot of new total proteome and unnormalized phosphoproteome that were conducted concurrently in the same platform. **G**. PCA plot of phosphoproteome normalized to total proteome. **H**. Heatmap of expressions of phosphoproteins normalized to total proteins. **I**. Volcano plot of normalized phosphoproteome. Red dots represent upregulated phosphoproteins with -log10(p-value) > 1.3 and log2(fold change) ⩾ 0.4; blue dots represent downregulated phosphoproteins with -log10(p-value) > 1.3 and log2(fold change) ⩽ -0.4; grey dots represent nonsignificantly regulated phosphoproteins with -log10(p-value) ⩽ 1.3 or absolute(log2(fold change)) < 0.4. **J**. Comparison of canonical pathway enrichments between

985 unnormalized and normalized phosphoproteome. Orange fill colors indicate that all comparable pathways
986 on the top are activated in both omics datasets. The darker the color is, the greater the absolute(z-score) is,
987 and the more significantly enriched the pathway is.

988

989 **Figure 6. Coordinated regulation of transcriptome, proteome and phosphoproteome on PI3K/AKT**
990 **and ERK/MAPK signaling pathways and protein synthesis and degradation. A**. Canonical pathway
991 enrichment of phosphoproteome only with cutoff p-value < 0.05. The darker the color is, the greater the
992 absolute(z-score) is, and the more significantly enriched the pathway is. **B**. Comparison of PI3K/AKT
993 signaling and protein ubiquitination pathways enriched from transcriptome (red outline), proteome (blue
994 outline) and phosphoproteome (green outline). **C-D**. Western blots of two phosphorylation sites on pan-
995 AKT protein for verification of phosphorylation and activation of PI3K/AKT signaling pathway in
996 TGAC8 vs. WT. **E**. Western blot of ubiquitination in TGAC8 vs. WT. **F**. Pathway graph of PI3K/AKT
997 signaling marked with changes in transcriptome (left box), proteome (middle box) and phosphoproteome
998 (right box). Fill colors indicate changes: red and green indicate upregulation and downregulation
999 respectively; grey indicates nonsignificant regulation. **G**. Phosphopeptide number of substrates of PI3K.
1000 Y-axis represents protein substates of PI3K; x-axis represents number of phosphopeptides. Red and blue
1001 bars indicate upregulated (p-value < 0.05 and log2(fold change) > 0) and downregulated (p-value < 0.05
1002 and log2(fold change) < 0) phosphopeptides respectively. Two-tailed unpaired Student's t test with
1003 Welch's correction was conducted and p-values were shown in plots.

1004

1005 **Figure 7. Analyses of proteins changed discordantly in proteome and phosphoproteome. A**. Venn
1006 diagram of significantly regulated proteins in total proteome and significantly regulated phosphoproteins
1007 in unnormalized phosphoproteome that were conducted concurrently in the same platform. **B-D**.
1008 Functional analyses of proteins whose expressions are changed discordantly at total protein and
1009 phosphorylation levels. Mitochondria and others are enriched in cellular component analysis (**B**).
1010 Functions related to metabolism, mitochondria and others are enriched in Reactome pathway (**C**) and
1011 biological process analyses (**D**).

1012

1013 **Figure 8. Deduced schematic of coordination of phosphoproteome with transcriptome and**
1014 **proteome in TGAC8 mouse LV.** Based on our results, we deduced a mechanism of reprogramed
1015 phosphoproteome in TGAC8 mouse LV: First, TGAC8 mouse induces a PKA dependent phosphorylation
1016 via AC8-cAMP-PKA axis. Many cytoplasmic proteins including TFs are thus phosphorylated and then
1017 transported into the nuclear where TFs recognize and bind to the promotors to activate the transcription of
1018 more regulatory factors, including kinases, phosphatases, and TFs. The activation states of these factors
1019 are changed upon phosphorylated in cytosol, thereby activating additional kinases-controlled
1020 phosphorylation cascades and reprogramming the cardiac phosphoproteome comprehensively. Left
1021 column: AC8-cAMP-PKA signaling; middle column: phosphorylation (phosphoproteome); lower right:
1022 transcription (transcriptome); upper right: translation (proteome).

1023

1024

Figures and Supplementary Figures

Figure 1. TGAC8 reprograms the LV phosphorylation state.

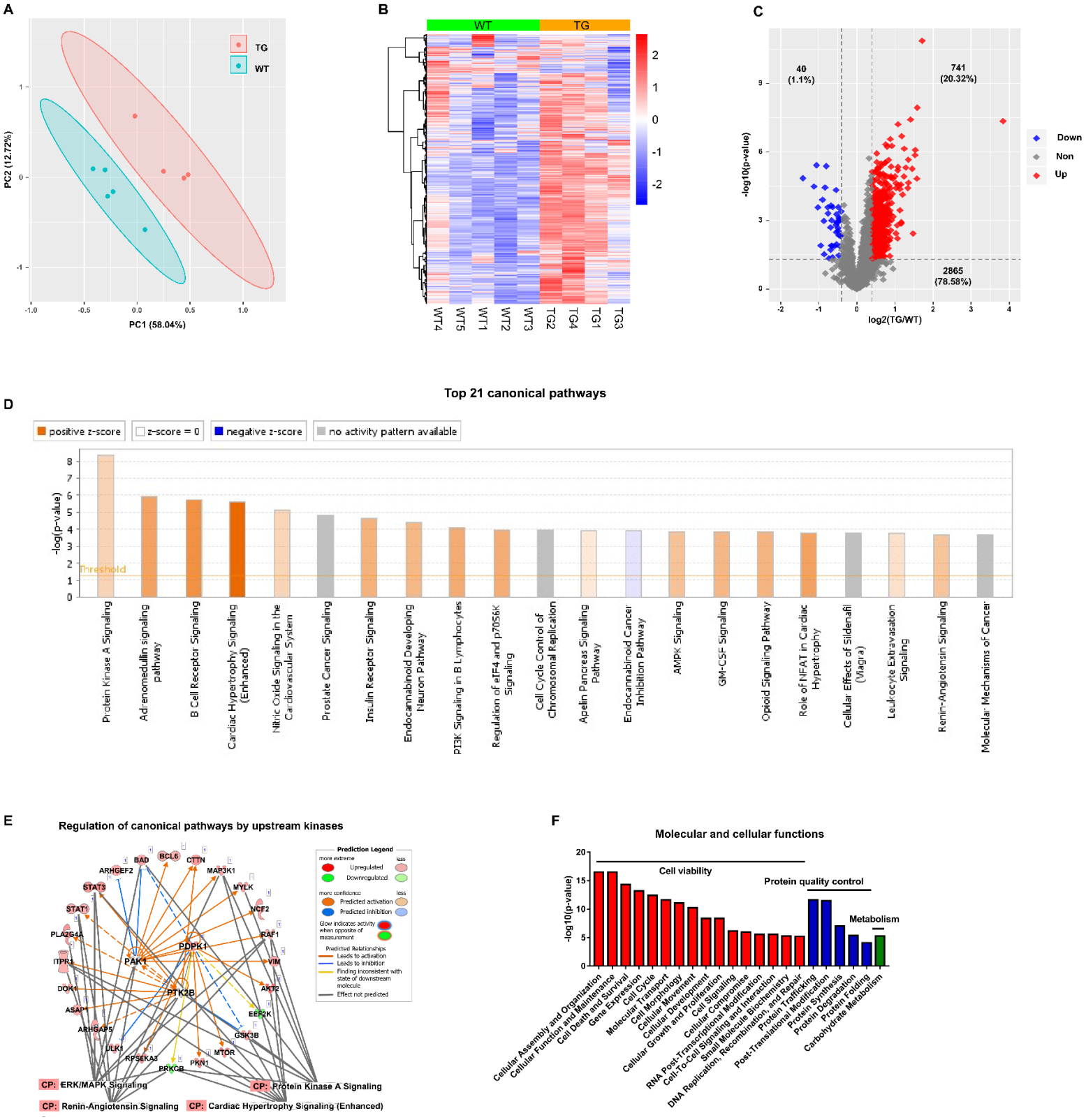

1028 **Figure 2. Characteristics of upregulated phosphopeptides.**

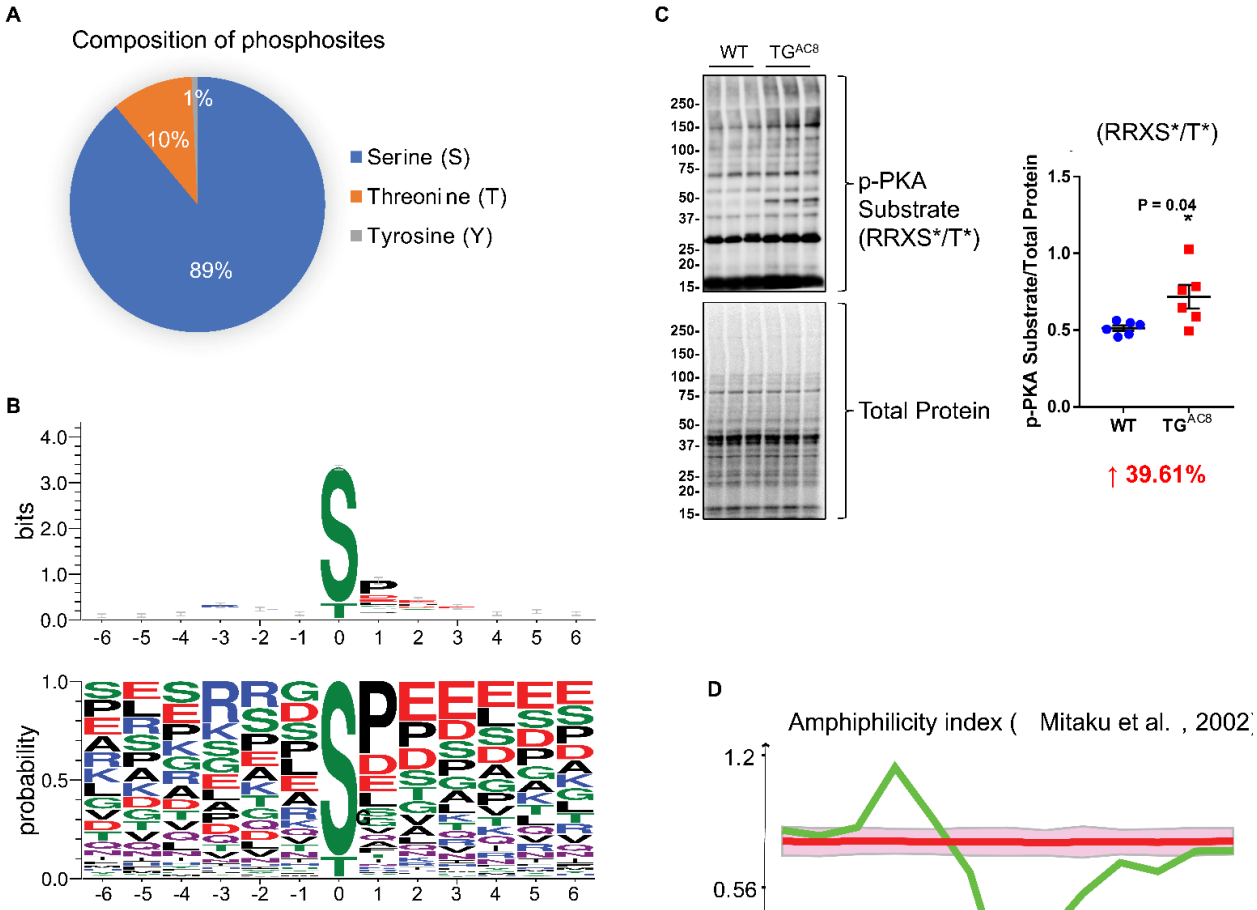

Polar	G,S,T,Y,C	green
Neutral	Q,N	purple
Basic	K,R,H	black
Acidic	D,E	red
Hydrophobic	A,V,L,I,P,W,F,M	black

1029

1030

1031

1032

1033

1034

1035

1036

1037

1038

Figure 3. Integrative analysis of transcriptome, proteome and phosphoproteome.

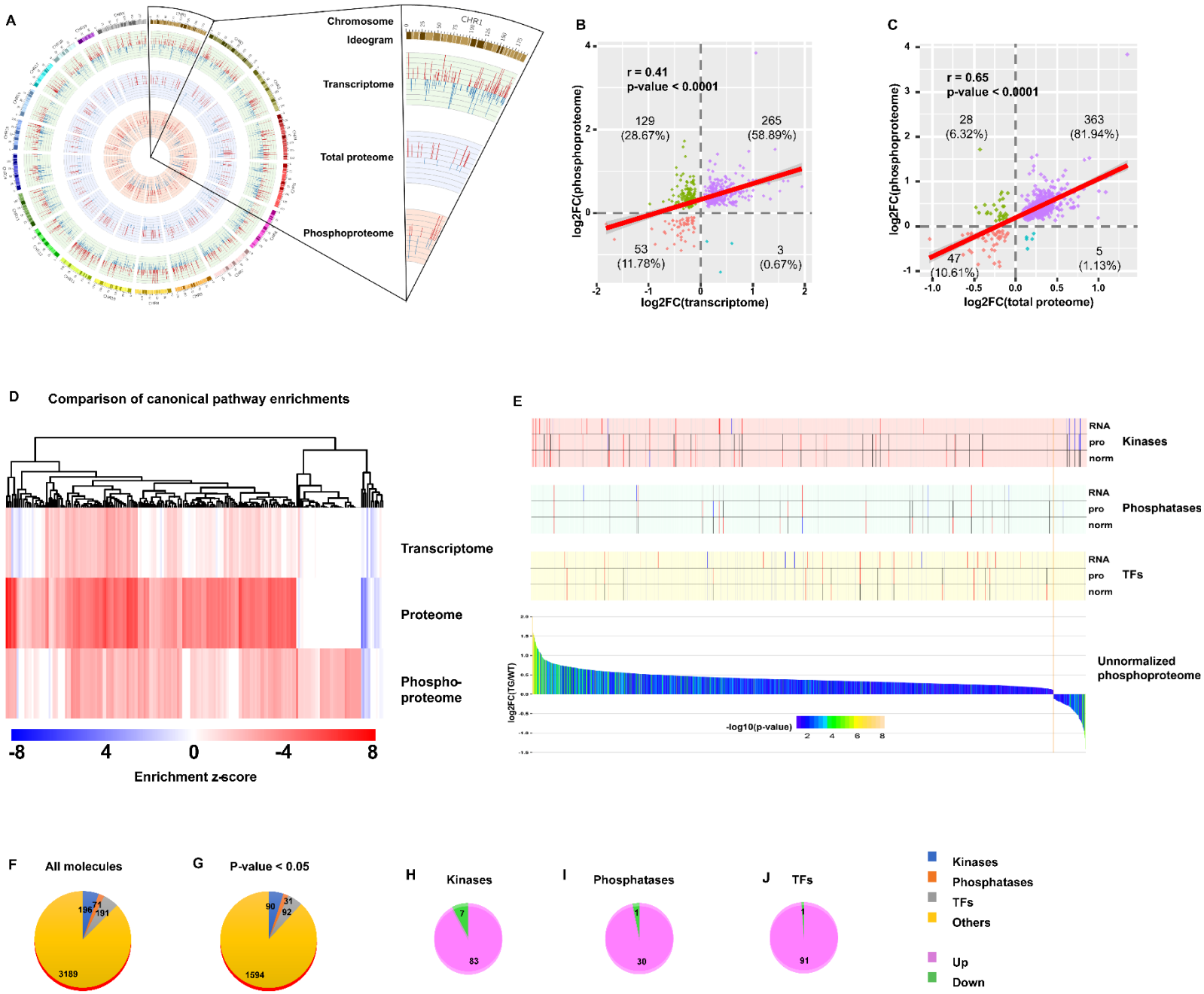

1046 **Figure 4. Coordination of phosphoproteome and transcriptome.**

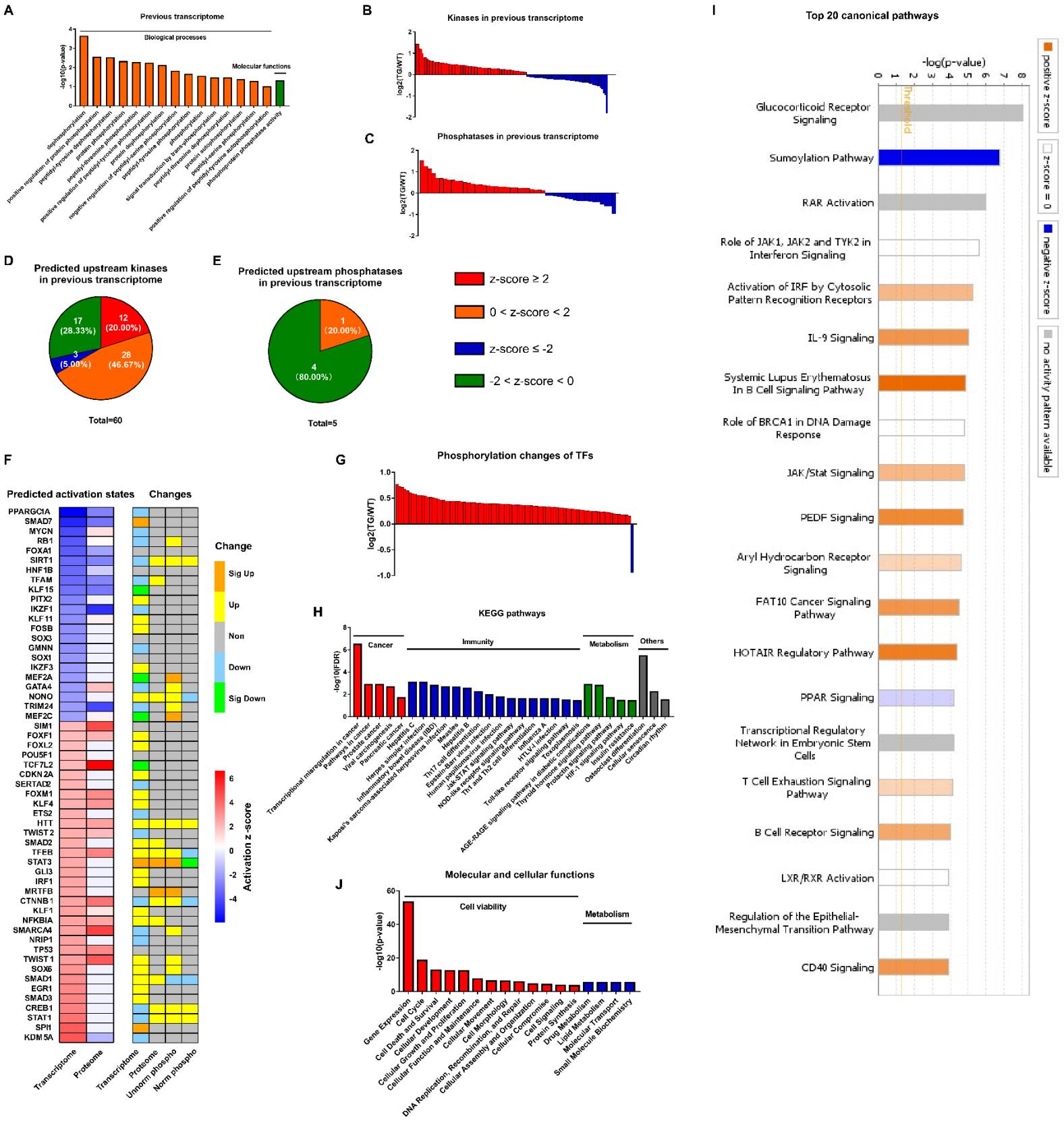

1048 **Figure 5. Analysis of normalized phosphoproteome.**

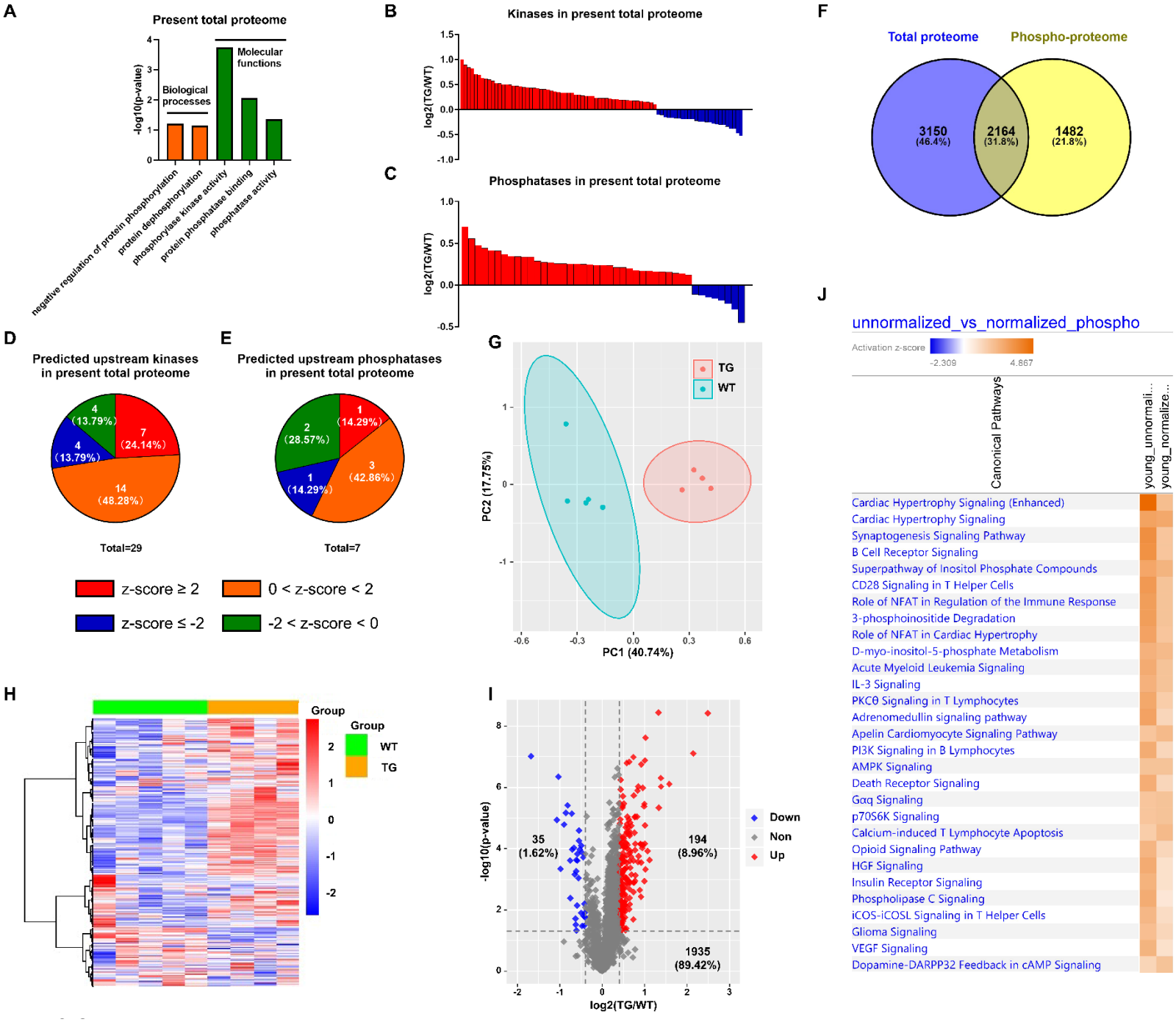

1050

1051

1052

1053

Figure 6. Coordinated regulation of transcriptome, proteome and phosphoproteome on PI3K/AKT and ERK/MAPK signaling pathways and protein synthesis and degradation.

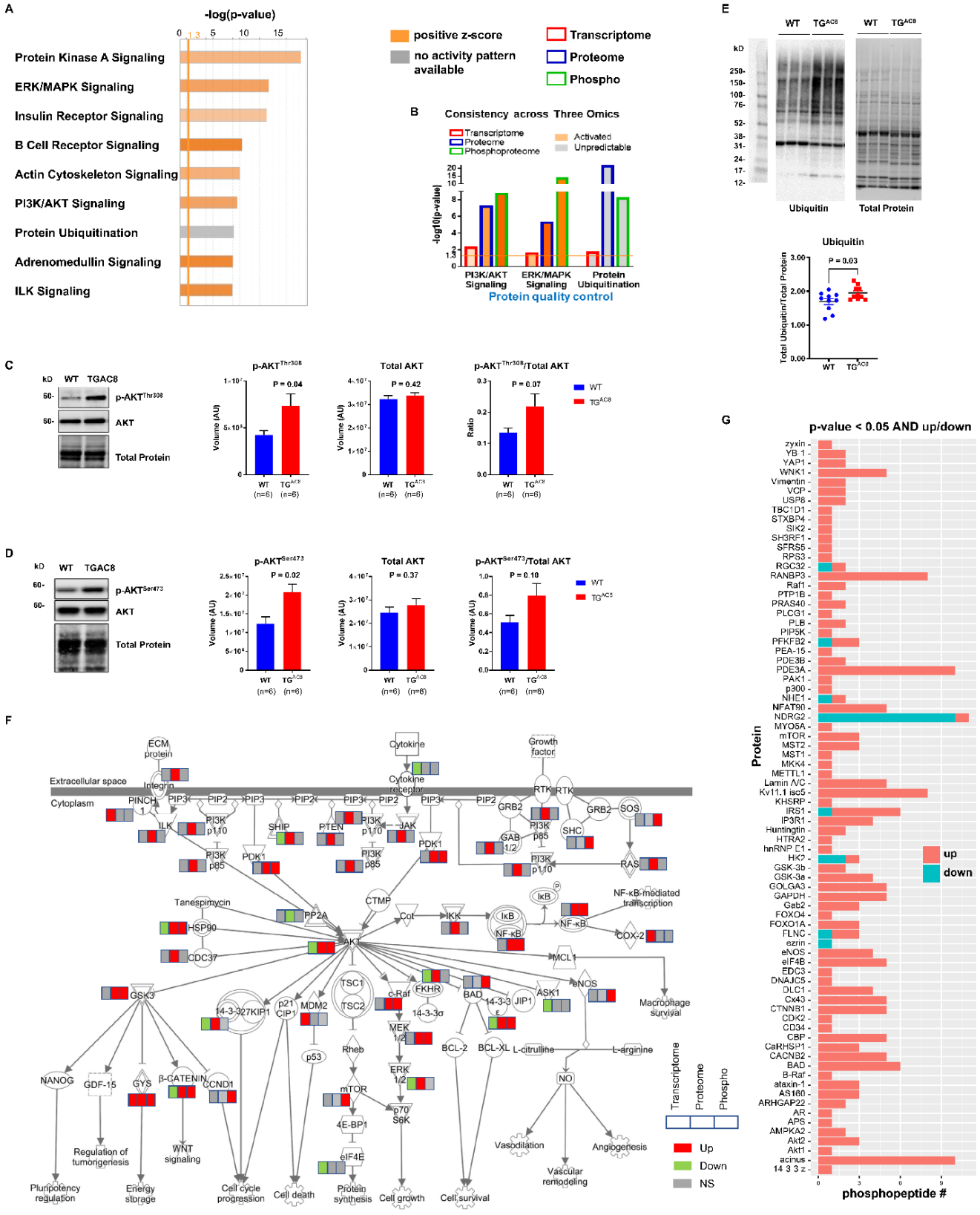

1057 **Figure 7. Analyses of proteins changed discordantly in proteome and phosphoproteome.**

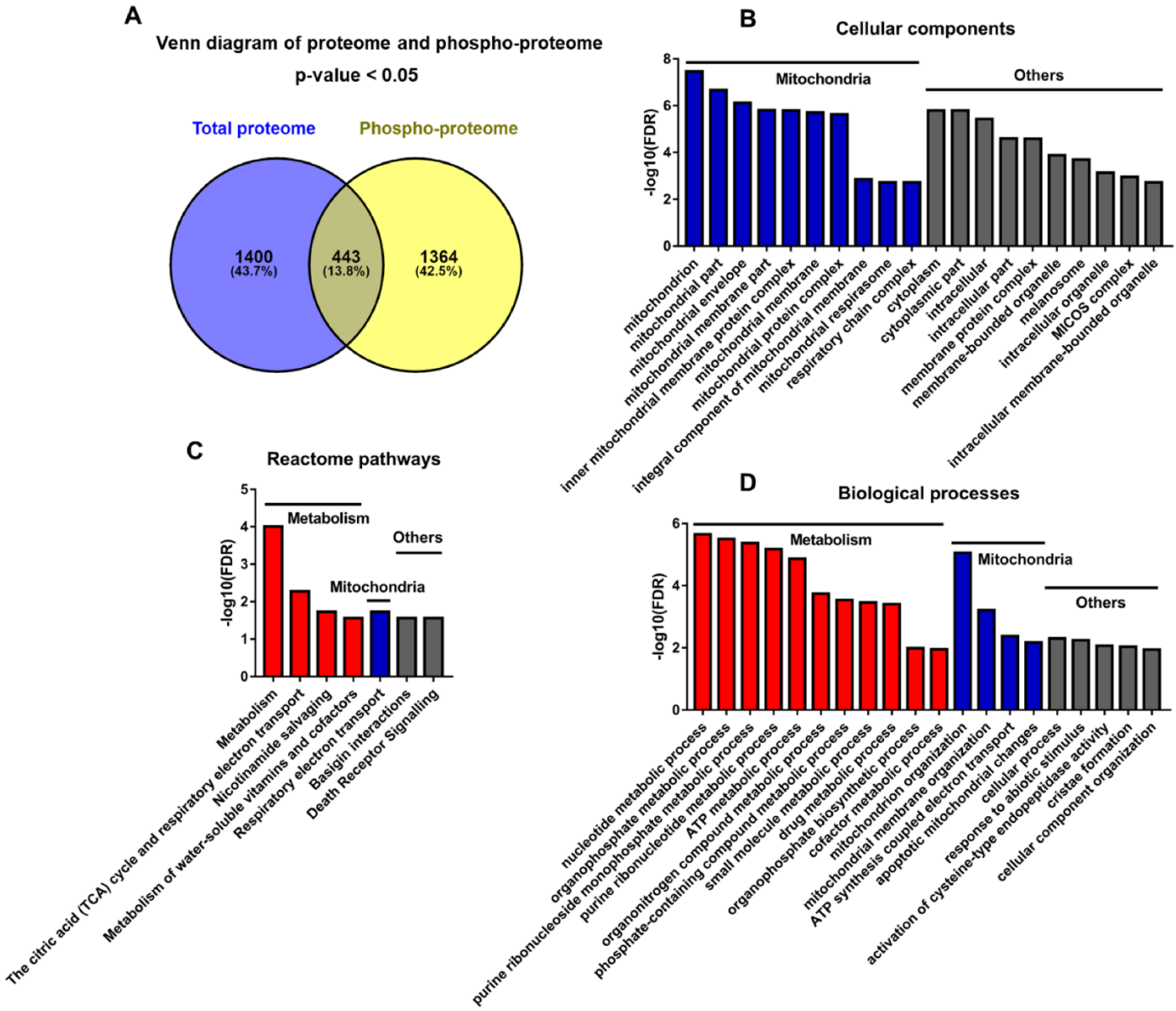

1059

1060

1061

1062

1063

1064

1065

1066 **Figure 8. Deduced schematic of coordination of phosphoproteome with transcriptome and**
1067 **proteome in TGAC8 mouse LV.**

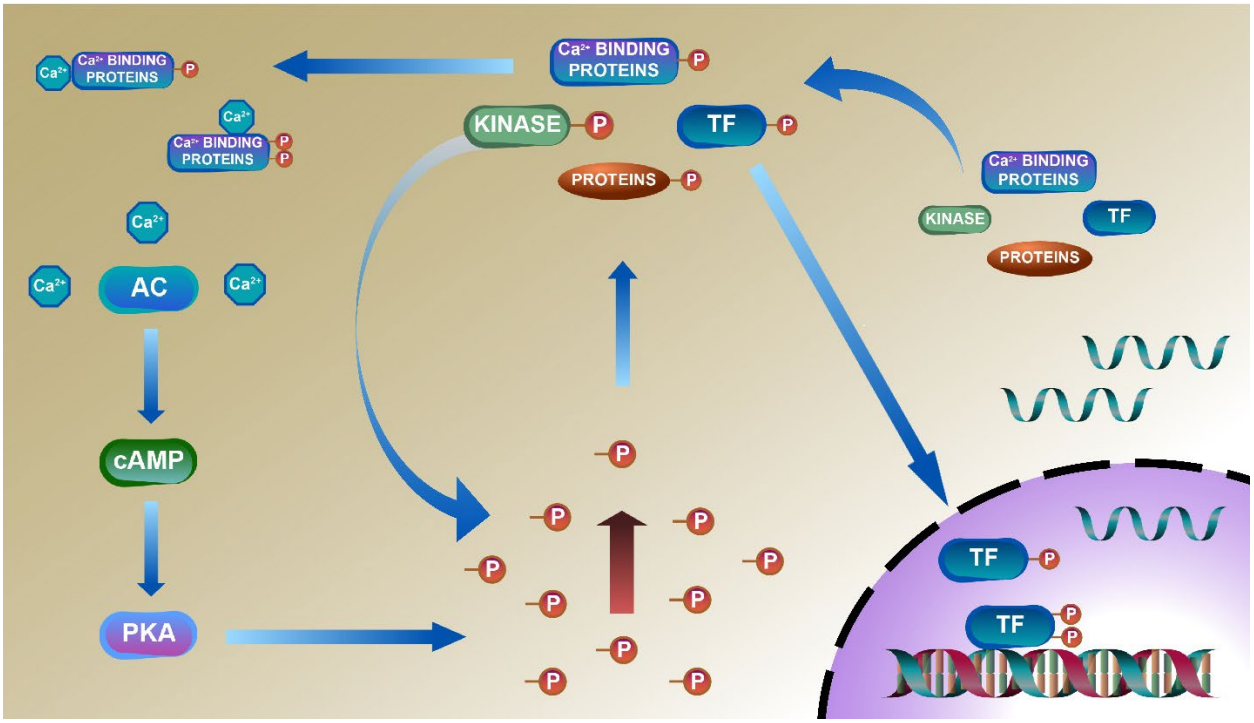

1068
1069
1070
1071
1072
1073
1074
1075
1076
1077
1078
1079
1080
1081
1082
1083

1084 **Supplementary Figure 1. The enriched pathway, Cardiac Hypertrophy Signaling (Enhanced), from the**
1085 **phosphoproteome.**

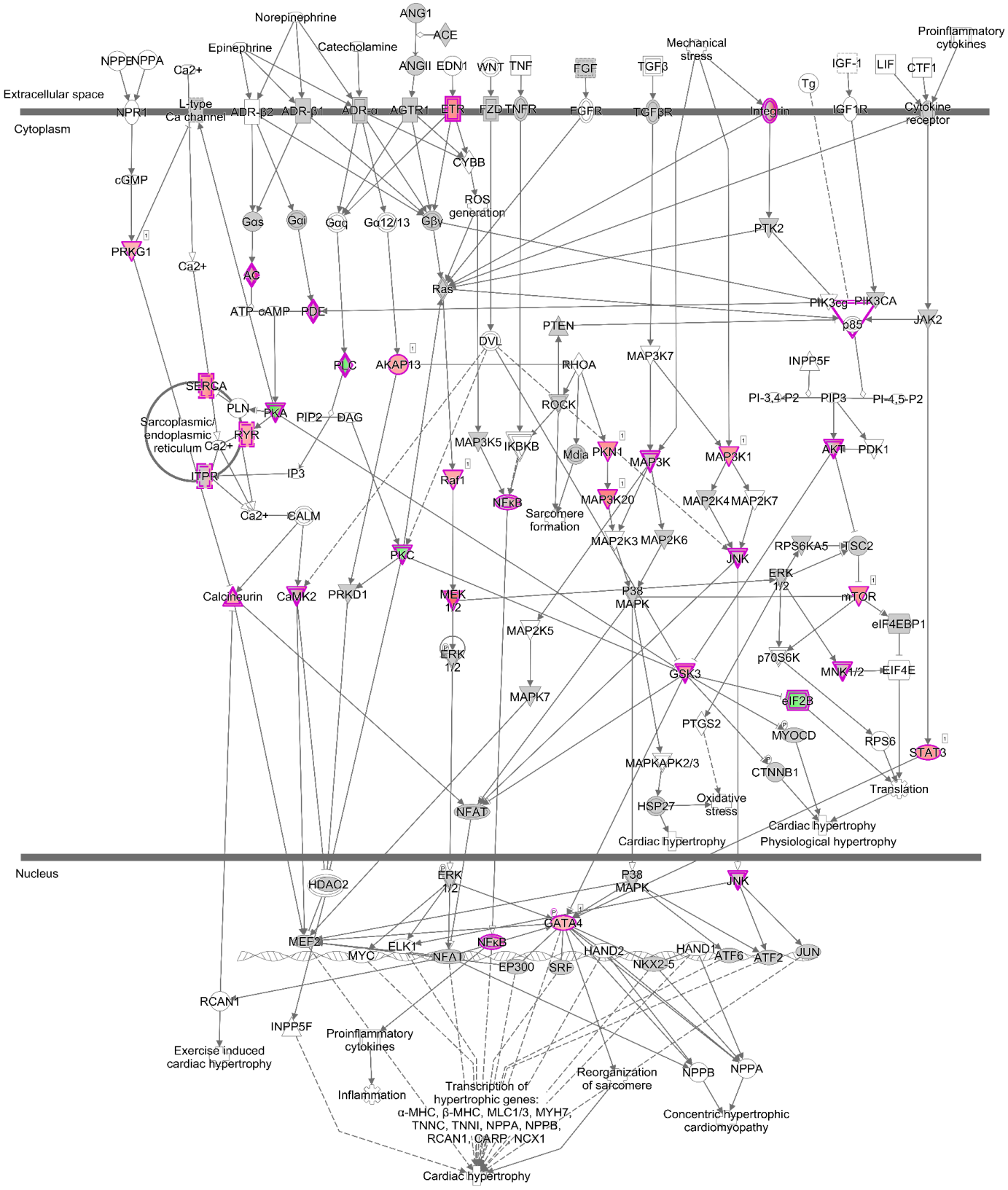

108

1087 **Supplementary Figure 2. The regulatory pathway under the control of a predicted upstream**
1088 **kinase, PDPK1.**

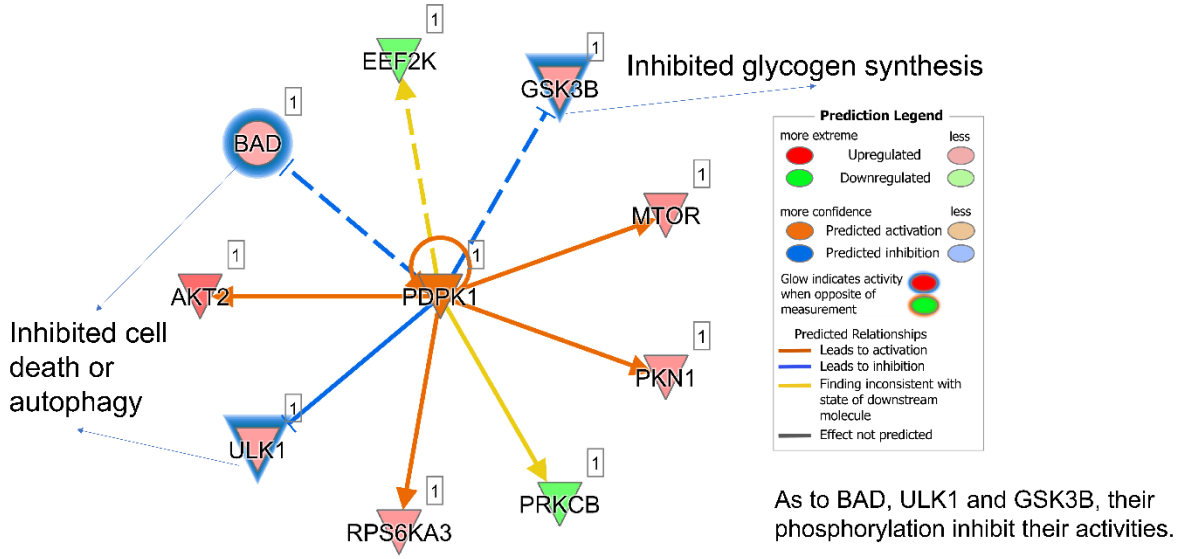

Symbol	Entrez Gene Name	UniProt	Log Ratio	p-value	Location	Family
AKT2	AKT serine/threonine kinase 2	Q60823	0.840825	0.007813	Cytoplasm	kinase
BAD	BCL2 associated agonist of cell death	Q61337	0.476462	7.81E-06	Cytoplasm	other
EEF2K	eukaryotic elongation factor 2 kinase	O08796	-0.42591	0.004744	Cytoplasm	kinase
GSK3B	glycogen synthase kinase 3 beta	Q9WV60	0.556065	0.002741	Nucleus	kinase
MTOR	mechanistic target of rapamycin kinase	Q9JLN9	0.640641	0.000144	Nucleus	kinase
PDPK1	3-phosphoinositide dependent protein kinase 1	Q9Z2A0	0.651174	0.02451	Cytoplasm	kinase
PKN1	protein kinase N1	P70268-2	0.600171	0.007485	Cytoplasm	kinase
PRKCB	protein kinase C beta	P68404-2	-0.44609	0.001011	Cytoplasm	kinase
RPS6KA3	ribosomal protein S6 kinase A3	P18654	0.580733	0.005794	Cytoplasm	kinase
ULK1	unc-51 like autophagy activating kinase 1	O70405	0.549454	0.015177	Cytoplasm	kinase

1089
1090
1091
1092
1093
1094
1095
1096
1097
1098
1099
1100
1101

1102 **Supplementary Figure 3. Cross verification of activated PI3K/AKT and ERK/MAPK signaling**
1103 **pathways and enhanced protein synthesis and degradation from our previous study.**

1104

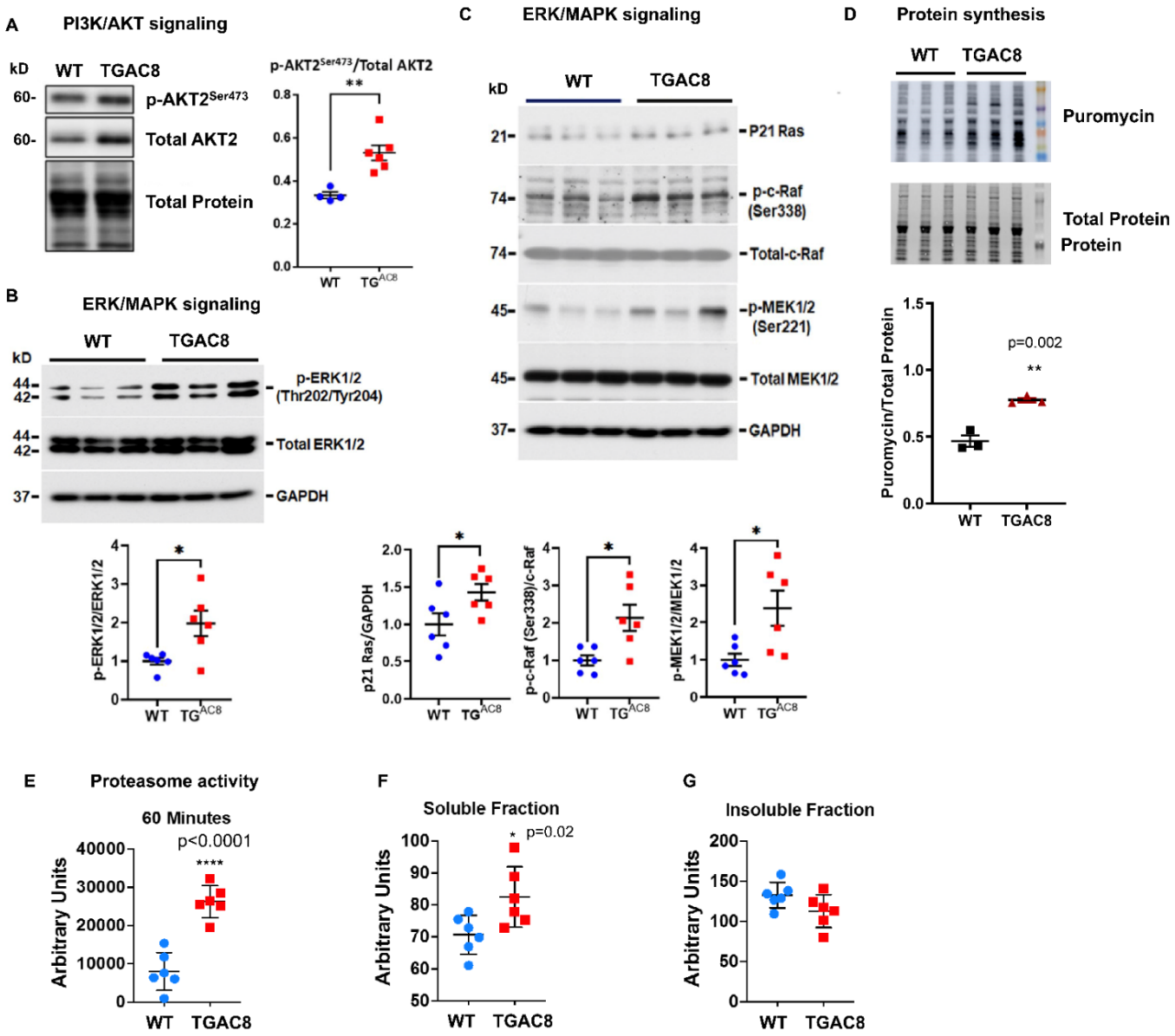

1105

1106

1107

1108

1109

1110

1111

1112 **Supplementary Figure 4. A comprehensive circuitry of TGAC8 mouse heart concluded from this**
1113 **phosphoproteome combine with previous transcriptome and proteome.**

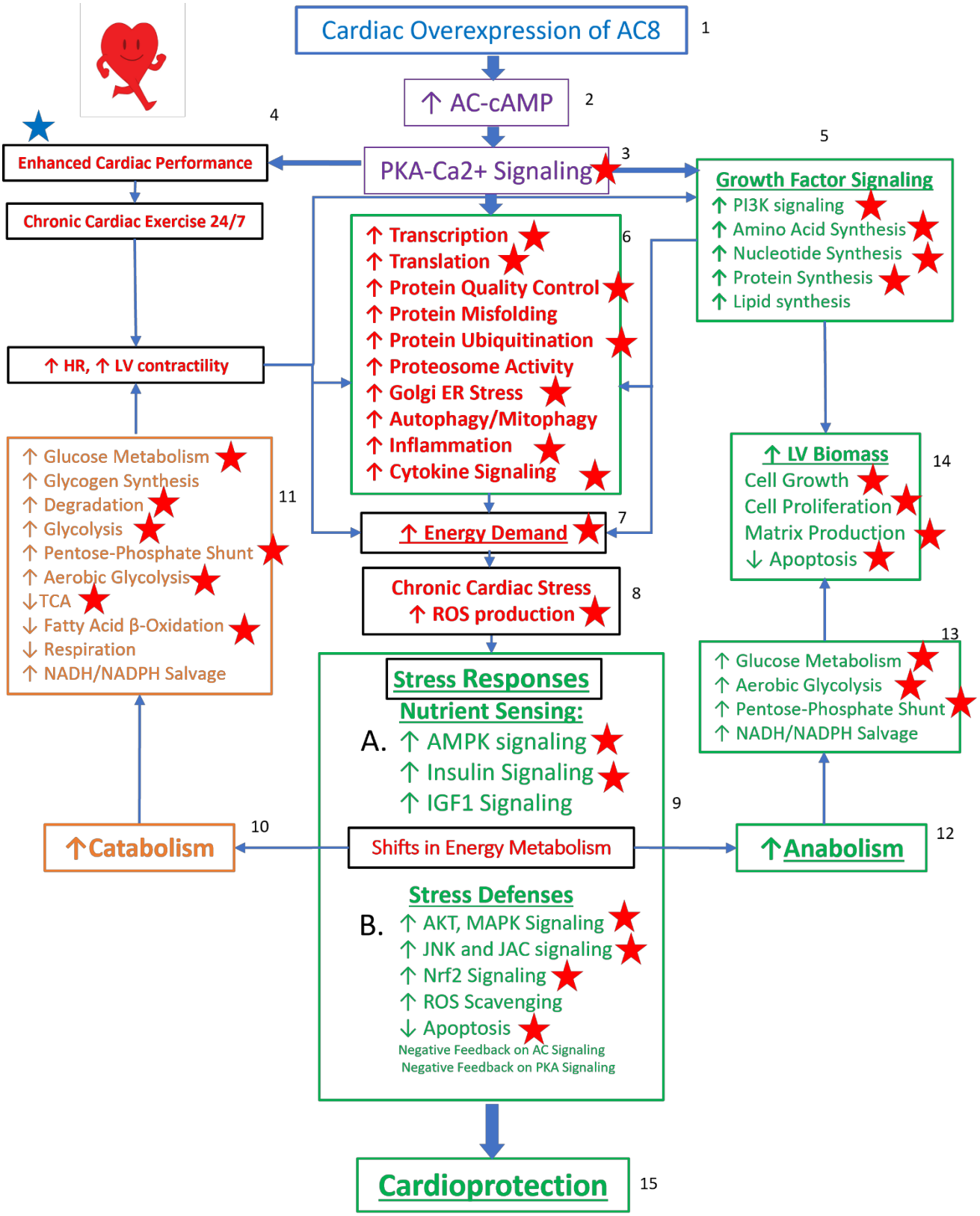

1114